Chapter Three:

In-situ Neutron-beam Diffraction Studies of the Palladium-Deuterium System:

Macroscopic Properties

Chapter Three:

In-situ Neutron-beam Diffraction Studies of the Palladium-Deuterium System:

Macroscopic Properties

3.1 Introduction

The experiments described in this thesis comprised neutron-beam diffraction studies of the peri-critical region of palladium-deuterium i.e. at temperatures near the palladium-deuterium critical temperature. In all experiments here the deuterium was introduced into the palladium from the gaseous phase. Both powdered palladium and sheet palladium samples were used, and there appear to be few observable differences between the deuterides of both forms. The bulk sample presented problems in full analysis of its diffraction patterns arising from preferred orientation in its crystal structure probably as a result from cold rolling.

It has been shown [2] that for hydrogen absorbing metals it is possible to get quantative information on the electronic density-of-states and the hydrogen concentration of the Fermi energy, directly from experimentally determined pressure-composition isotherms.

3.2 Sample Preparation

Differing sample surface conditions have presumably caused differences in the measured physical parameters of palladium-hydride in the past, mostly those of electrolytically charged palladium, but occasionally those involving gaseous charging.

Care was taken with all samples in this study to reduce their exposure to oxidizing atmospheres. This usually involved loading and sealing the powdered palladium samples into the sample cell under an argon atmosphere via a glove bag. The samples were then vacuum heated to at least 300°C and then exposed to less than an atmosphere of hydrogen for a minute.

or two to reduce any oxides adhering to the sample surface. The sample was then left at temperature under vacuum for a period not less than three hours, and then sealed under vacuum or argon until the diffraction experiments were started.

Note that earlier experimenters working with bulk palladium samples found that surface impurities, including oxides, were necessary to aid the absorption of hydrogen[3, 4]. Worsham et al in fact state that exposing a palladium sample to argon (as we did) at 450°C greatly reduces its ability to absorb hydrogen. This was not observed in the experiments of this thesis, though the kinetics of absorption were not studied. As it is specific active sites on the palladium-surface that catalyse the dissociation of hydrogen molecules into hydrogen atoms prior to absorption, it would be assumed that surface impurities would block absorption. The same sites catalyse the re-association of hydrogen atoms into hydrogen molecules.

Lewis [5] catalogues a number of methods for pre-treating a palladium surface, though states that these methods are empirically based, and not universally agreed upon. Bombardment of the surface with argon ions has proved successful on a number of occasions. Another method proved useful is repeated cycles of electrolytic charging followed by temperature-swing discharging (heating to redness).

Research into the use of palladium membranes for hydrogen separation supports the view that the dissociative properties of palladium and palladium-alloys towards hydrogen, and by association the sorptive properties, are deteriorated by many impurities, including specifically carbon-monoxide and sulphur. These poisons block the catalytic-dissociation sites on the surface of the palladium, stopping the dissociation of the hydrogen molecule into atomic hydrogen, the crucial first step to absorption.

The recent view is that air oxidations helps to clean the surface of impurities, improving hydrogen flux [10]. Oxidation also changes the surface morphology, which may help increase hydrogen absorption. Studies of palladium membranes have found that coating the surface with palladium-black to increase surface-oxidation has proved successful in increasing the activation of the surface to the dissociation and re-association of hydrogen. The same technique could be used for surface preparation of palladium sheets prior to low temperature sorption experiments.

Palladium-copper alloys undergo a phase transformation from body-centered-cubic structure to face-centered-cubic structure at elevated temperatures, and this phase change correlates with a transition from sulphur-poisoning to sulphur-tolerance in a membrane

3.3 HIFAR MRPD October 2001

A solid sheet of 99.999% pure palladium weighing 12.866 g was loaded into a stainless steel lined TiZr high pressure sample cell. A solid solution of titanium-zirconium in the correct molecular proportions produces a "null-matrix" which will scatter neutrons only very, very weakly. The thin stainless-steel lining is to prevent hydrogen embrittlement of the TiZr, and is as thin as possible so as to minimize the amount of stainless steel in the scattering cross-section of the neutron beam. The palladium sheet was rolled into a spiral cylinder in an attempt to counteract the effects of preferred orientation in the sample.

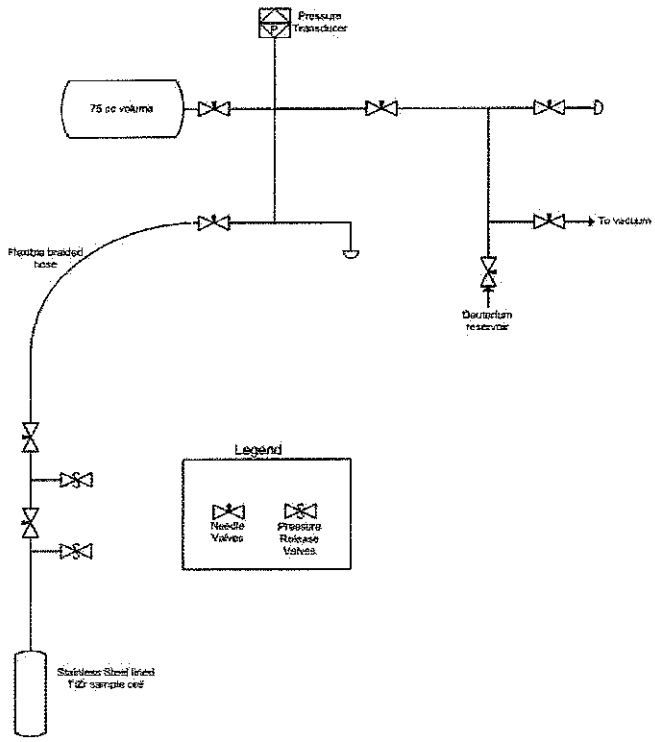

Fig 3.1 Schematic of Sieverts apparatus used for experiment of October 2001

The Sieverts apparatus used for the experiment is shown as a schematic 'piping and instrumentation' (P&I) diagram in Fig 3.1. The total system volume, without sample, was 164.34 cc, calibrated relative to a 305.6 cc reference volume that had been calibrated with distilled water.

The kinetics of absorption at all three temperatures was very fast, with equilibrium seemingly achieved within a few minutes of changing the sample pressure. Regardless, each pressure step in the following isotherms was left for a minimum of 1 hour to equilibrate.

3.3.1 Supercritical Isotherm

The first isotherm was traversed in absorption at a temperature of 300°C based on the critical temperature as reported by [11] This temperature was expected to be sufficiently above the T_{crit} to be wholly in the single phase portion of the palladium-deuterium phase diagram, while still presenting attainable gas pressures for the experimental apparatus used The isotherm is shown in Fig 3.2, each triangle on the graph representing a pressure step and a diffraction pattern

The isotherm displays a shape expected from a temperature close above the critical temperature There is no plateau region observable

Fig 3.3 shows the set of diffraction patterns collected from the super-critical isotherm The patterns have been displaced along the Count-axis for ease of viewing These all appear to be simple single-phase diffraction patterns and were treated as such. If a two-phase region has been traversed in the vicinity of deuterium concentrations 0 27 to 0.37 then the resolution of MRPD, along with the preferred-orientation problems of the sample, have ensured that will not be resolvable from these patterns See sections 3.5 and 3 6 for further insights to the imprecision of the critical temperature.

To remove the deuterium from the palladium sample, the deuterium reservoir was cooled in liquid nitrogen and then opened to the sample. The reservoir absorbed deuterium to an equilibrium pressure less than 5 kPa over a few minutes The reservoir was then closed, and the sample opened to vacuum and left as such as the furnace temperature was reduced to a temperature of 280°C over approximately one hour This was deemed sufficient to desorb all traces of deuterium from the palladium.

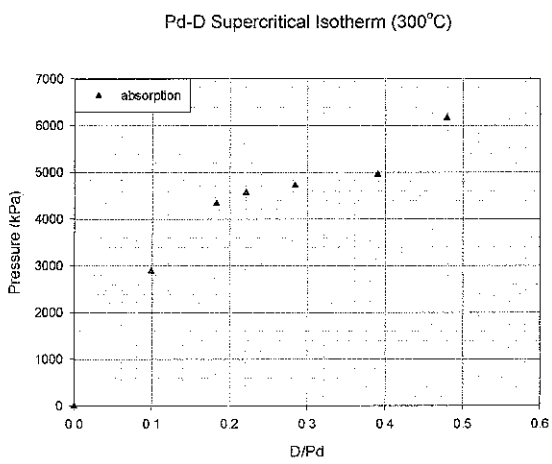

Fig. 3.2: Pd-D Supercritical (300°C) isotherm

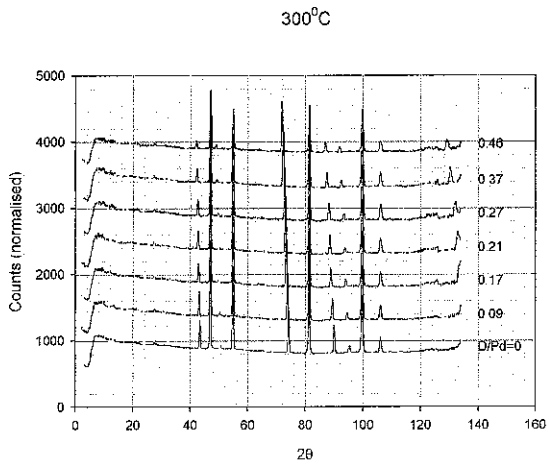

Fig 3.3: Pd-D Supercritical (300°C) diffraction patterns

3.3.2 Critical Isotherm

The second isotherm was traversed in absorption and desorption at a temperature of 280°C. This was expected to be as close to the critical temperature as possible. The isotherm is shown in Fig 3.4, the blue up-pointing triangles on the graph represent an absorption step and diffraction pattern, while the red down-pointing arrows represent a desorption step and diffraction pattern.

The isotherm displays a shape closer to that expected from within the two-phase region than was expected. The plateau region appears more pronounced than a mere inflexion point, though it is difficult to tell if hysteresis exists between the absorption and desorption parts of the isotherm. The patterns collected during this isotherm are shown in Figure 3.5. The patterns have been displaced along the Count-axis for ease of viewing. There is some evidence of a two-phase pattern based on the splitting of some of the higher angle palladium peaks in the pattern recorded at D/Pd=0.22 (Fig. 3.5).

It is thought then that the system did pass through a two-phase region during traversal of the isotherm at 280°C based on the evidence of Fig 3.5. Unfortunately, the sample had a very large preferred orientation evident in the diffraction patterns, as a result of cold rolling. This made it

impossible to refine the patterns to their full extent, and only lattice parameter data was obtained (see Chapter 4).

Only one phase could be refined from the critical temperature patterns, and this may be a combination of the following factors

- Insufficient resolution on MRPD
- Preferred orientation in the sample crystal structure
- Looking at Fig 3 4, it is possible that any two-phase region lies on a small plateau between the two data points at D/Pd=0.23 and D/Pd=0 32 so that a definitive two-phase patterns was not collected

This is unfortunate, as a definitive two-phase pattern here would have helped immensely in answering some questions regarding the value of the critical temperature, and its relationship to the form of the bulk palladium used.

To remove the deuterium from the palladium sample, the deuterium reservoir was cooled in liquid nitrogen and then opened to the sample The reservoir absorbed deuterium to an equilibrium pressure less than 5 kPa over a few minutes The reservoir was then closed, and the sample opened to vacuum and left as such as the furnace temperature was reduced to a temperature of 250°C over approximately one hour This was assumed sufficient to desorb all traces of deuterium from the palladium.

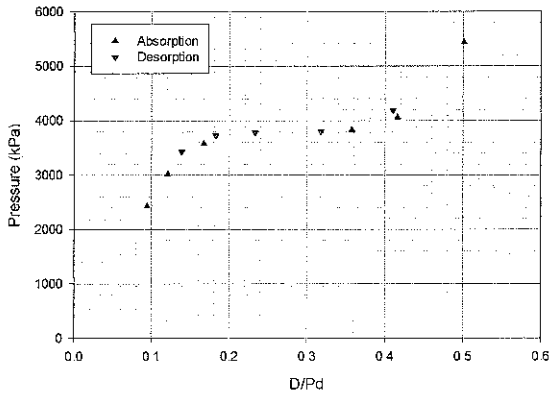

Fig 3 4: Pd-D critical temperature (280°C) isotherm

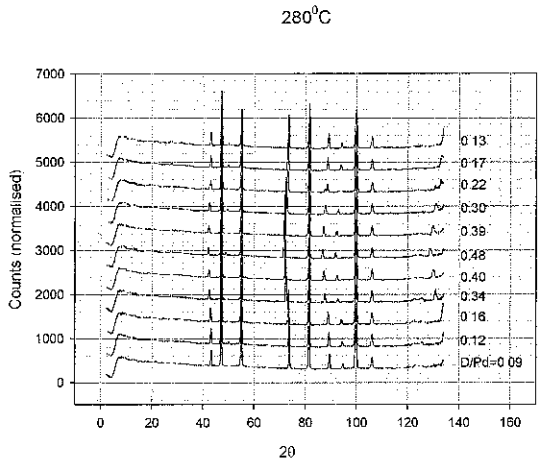

Fig 3.5: Pd-D critical temperature (280°C) diffraction patterns

3.3.3 Subcritical isotherm

The last isotherm traversed was at a temperature of 250°C. This was expected to be slightly below the critical temperature. The isotherm is shown in Fig 3.6, the blue up-pointing triangles on the graph represent an absorption step and diffraction pattern, while the red down-pointing arrows represent a desorption step and diffraction pattern

The isotherm displays characteristics of a two-phase pattern, with a distinct plateau region, and obvious hysteresis between the absorption leg and the desorption leg. Inspection of the diffraction patterns in Fig. 3.7 show two phase patterns developing in the absorption phase at deuterium concentrations of 0.29 and 0.34. Two-phase patterns also develop in the desorption phase at 0.31 and 0.25. Note that the diffraction patterns have been displaced along the Count-axis for ease of viewing

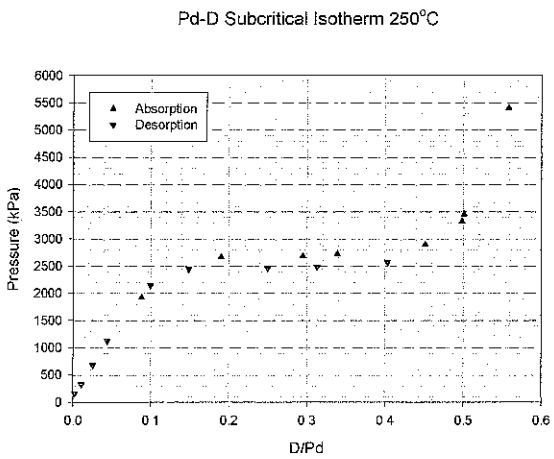

Fig 3.6: Pd-D sub-critical temperature (250°C) isotherm

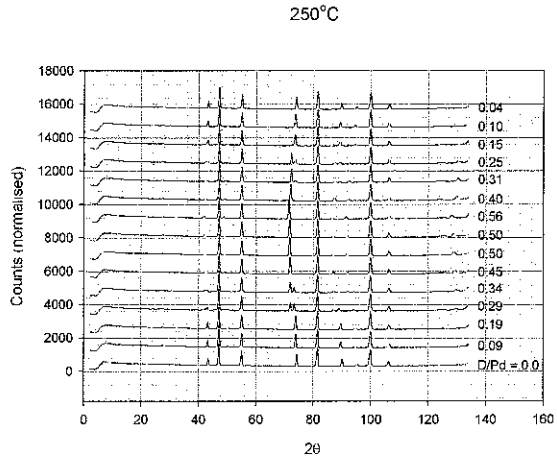

Fig. 3.7: Pd-D sub-critical temperature (250°C) diffraction patterns

3.3.4 The Peri-critical Region of the Palladium-Deuterium System

Fig 3 8 shows all the results from the experiments of November 2001 on the same graph, presenting a picture of the peri-critical region of the palladium-deuterium system and the beginnings of a phase diagram Based upon values quoted in the literature for the critical point of palladium-deuterium, and the results presented above and elsewhere in this thesis (see sections 3 5 and 3.6), an empirical estimate has been made of the possible extent of the single-phase/two-phase boundary. This boundary will lie somewhere in the blue shaded area shown on the graph

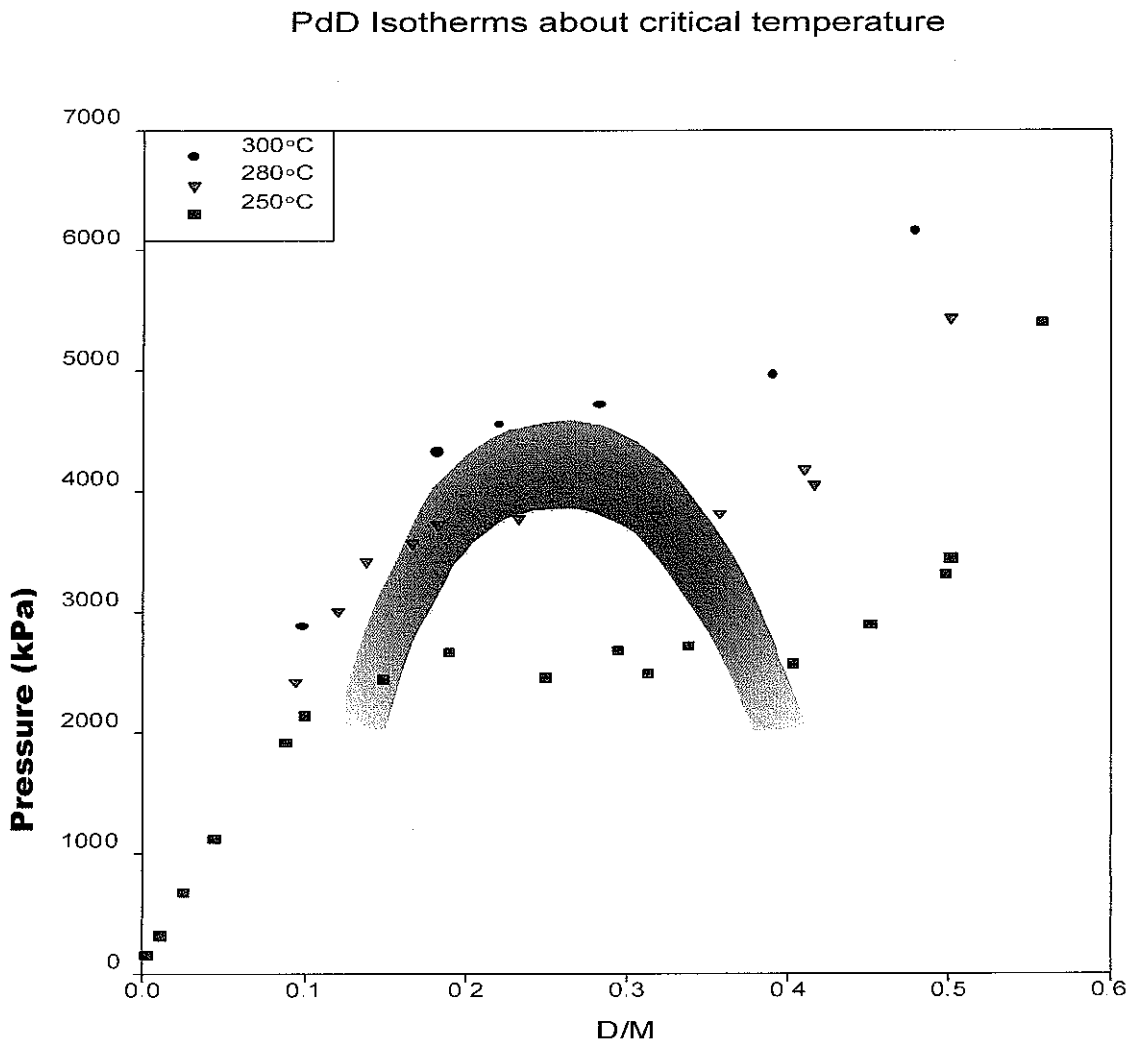

Fig 3 8 The peri-critical region of the palladium-deuterium system Isotherms are: filled black circles (300°C), red triangles (280°C), green squares (250°C) The blues filled area represents the estimated uncertainty in the single-phase/two-phase boundary based upon past-estimates and data presented in this thesis The actual two-phase boundary lies somewhere in this shaded area

Fig 3 9 shows the results from October 2001 on the same axes as results from [1], showing excellent agreement between both. The two 300°C isotherms are very close, neither exhibiting any plateau region around the critical point. The 250°C and 280°C isotherms fit nicely with the 270°C isotherm, and along with the 300°C isotherms, illustrate the evolution of the isotherm from the sub-critical to the super-critical. Note that as the temperature increases from the sub-critical, both the hysteresis and plateau regions of the isotherms diminish as the critical temperature is approached, and disappear completely above the critical temperature.

3.4 SINQ HRPT May 2002

The experiment carried out on the SINQ HRPT instrument at the Paul Scherrer Institute, Switzerland in May 2002 had the aim of explicitly trying to detect the occupation by deuterium of tetrahedral positions in the FCC palladium lattice (see Chapter 5). In this aim it was unsuccessful due to a number factors, though some of the results were salvaged for inclusion in Chapter 4.

3.4.1 Manometrics

The Sieverts apparatus used in this experiment is shown in Fig 3.10. The only palladium sample that could be obtained for this experiment was a previously handled sample obtained from Professor Klaus Yvon of Geneva. The state of this sample was completely unknown, it had not been touched in some ten years, and was possibly heavily oxidised. The poor results from this experiment are probably, in some ways, a result of the unknown status of this sample.

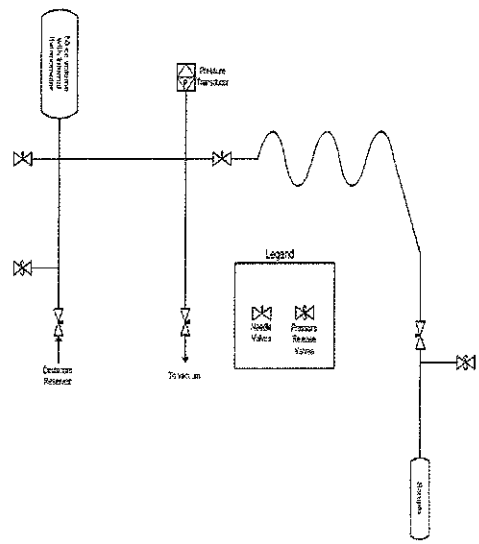

Fig. 3.10. Schematic of Sieverts apparatus used on SINQ HRPT May 2002

The desired manometics for this experiment were essentially those finally completed successfully at ISIS, Rutherford Appleton Laboratory in April/May 2004. That is, after annealing, the sample has to be taken through a super-critical isotherm, followed by a sub-critical isotherm, and then finally another super-critical isotherm, in order to induce the hoped for tetrahedral occupation.

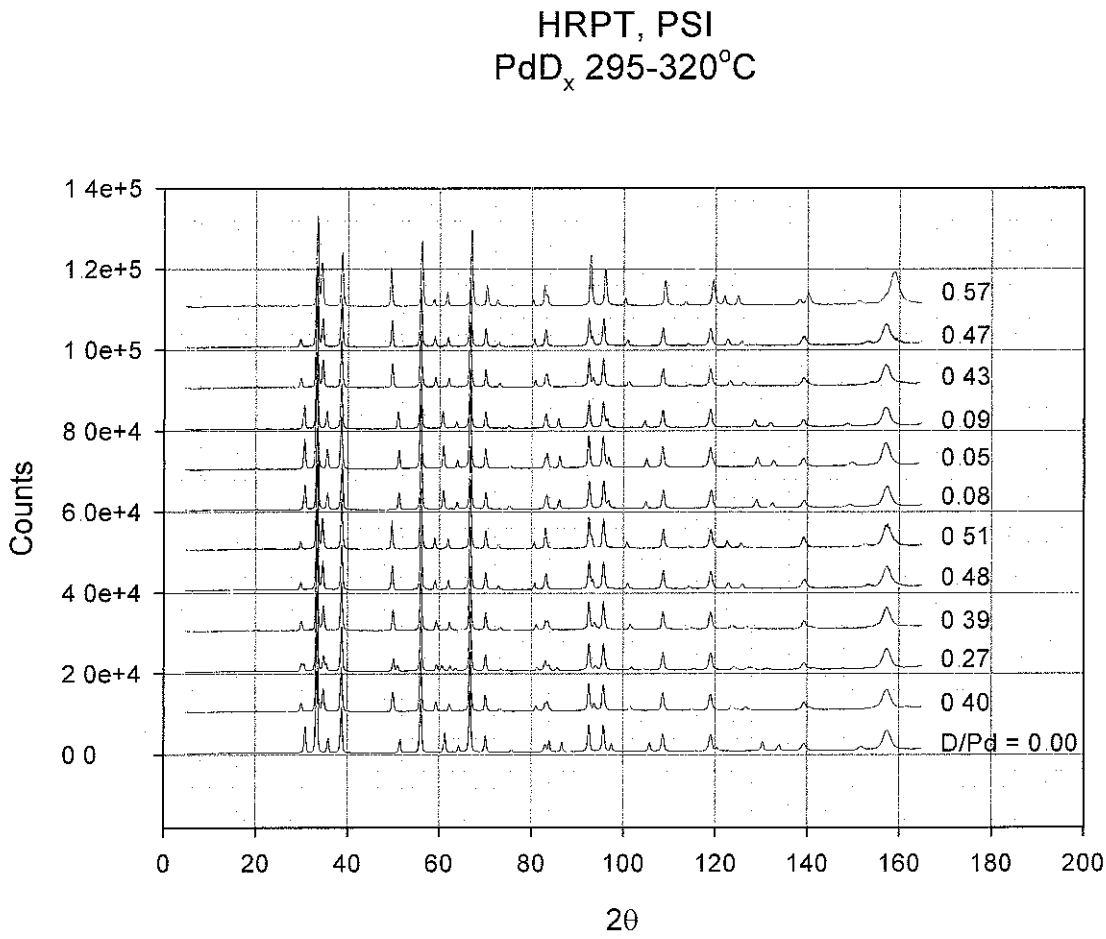

Fig 3.11: Neutron-beam diffraction patterns from palladium-deuterium collected on SINQ HRPT at PSI, Switzerland. Black patterns at ~295°C, red patterns at ~320°C, blue patterns at 120°C

Unfortunately, the manometics here did not work. Twice during the experiment the zero of the p-c-T diagrams were lost, and the D/Pd ratio had to be estimated and "pinned" at certain values. The first two isotherms, one at approximately 295°C and a second at approximately 320°C with a quench step to 120°C at the highest pressure point, were executed before losing

the zero and were used to extract lattice-parameter details for inclusion in Chapter 4 (section 4.4).

Fig 3 11 shows the patterns collected on HRPT during the first two isotherms The deuterium-to-palladium concentration listed beside each pattern were determined from the Rietveld refinements of the patterns, not via the Sieverts technique.

3.5 HIFAR MRPD July 2002

The aim of this experiment was two-fold The first aim was to see if high deuterium gas pressure (100 - 700 bar) at room temperature was sufficient to cause occupation of tetrahedral sites in a new palladium sample The second aim was to see if long-range ordering of the beta-phase palladium-deuterium could be detected through the observation of low-count, high d-spacing super-lattice peaks in the neutron diffraction patterns

3.5.1 Manometrics

The sample used was a previously un-handled sample provided by Dr R. Thomas Walters of the Savannah River Company. The morphology of this sample was somewhat unique, resembling a bunch of grapes, with the individual 'grape' size being only a few microns This imbued the palladium with a very low *tapping density* and the mass of the sample was therefore only 5 827 g, limited by the internal dimensions of the sample-cell

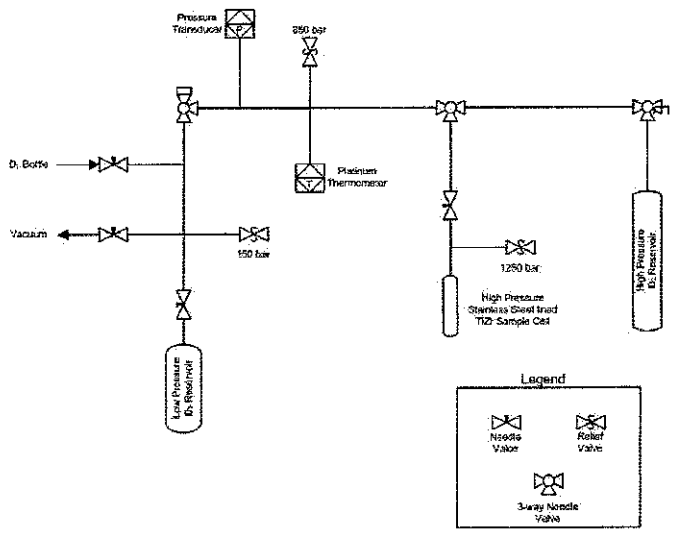

Fig 3 12. Schematic of Sieverts apparatus used on HIFAR MRPD July 2002

A schematic of the Sieverts apparatus used in this experiment is shown in Fig 3 12. The total system volume of the high-pressure section

of this hydrogenator, without sample, was 35.67 cc. The entire high-pressure section was wrapped in bubble-wrap to insulate it from ambient temperature fluctuations.

Fig 3.13 plots the pressure-composition points calculated during the experiment. Judging by the erratic nature of the isotherm points, insufficient care was taken with the apparatus to allow it to equilibrate during absorption of the deuterium. Fig 3.14 shows the diffraction patterns collected during the experiment, taken at the points on the isotherm marked by red circles. A slow leak developed in the one of the fittings between the sample cell and the pipe feeding it. This was not detected until the final point of the isotherm, at which time the leak was removed by gently tightening the leaking fitting. This means that the highest concentration stated for the isotherm (D/Pd=0.78) is slightly exaggerated.

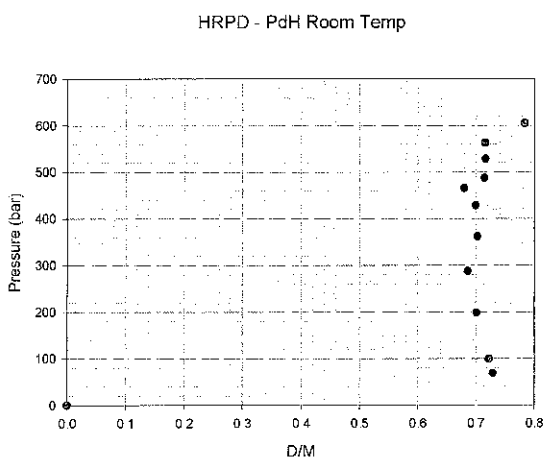

Fig. 3.13 Room temperature p-c-T diagram for palladium-deuterium. Red dots indicate points where diffraction patterns were collected.

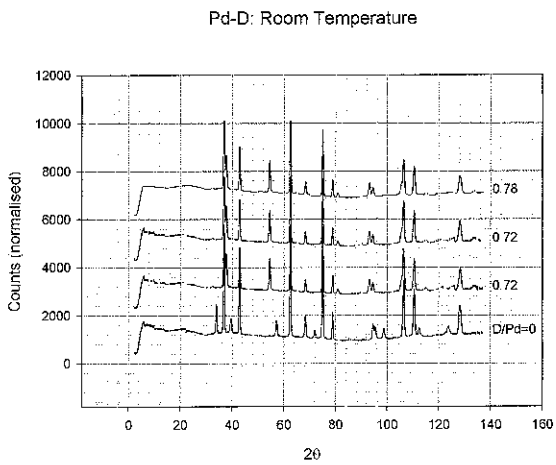

Fig 3.14 Room-temperature neutron-beam diffraction patterns of palladium-deuterium. The two patterns at D/Pd = 0.72 are not a repeat, the concentrations have rounded to two decimal places.

3.5.2 Instrument Calibration Problems

This experiment was marred by problems correcting for the erratic background of the diffraction patterns. This was caused by incorrect calibration of MRPD and could not be

corrected for. Therefore, again, only lattice parameter data could be extracted from Rietveld analysis of the diffraction patterns (see Section 4.4).

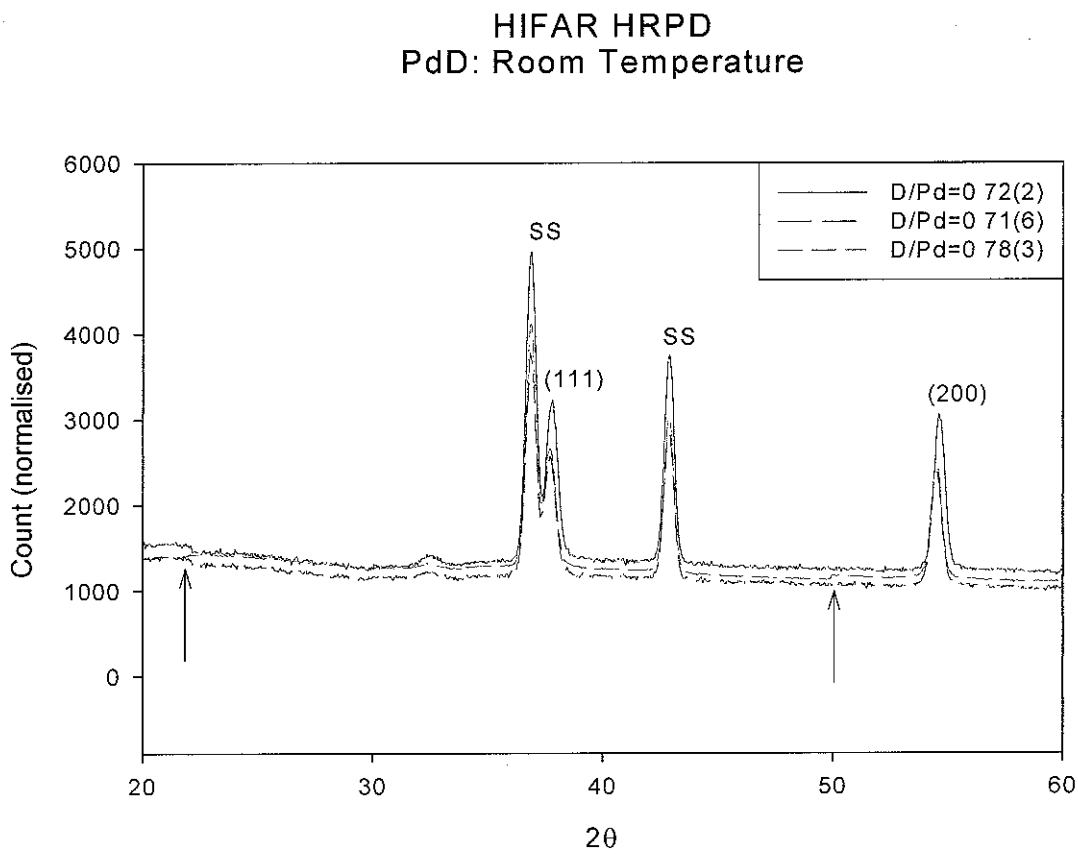

Fig 3.15. Detail of diffraction patterns of Pd-D collected on HIFAR MRPD July 2002

The plots shown in Fig 3.15 are details of 3 of the patterns shown in Fig 3.14. The digit in the brackets listed after each deuterium concentration is the uncertainty in that concentrations last digit. The patterns have been scaled to the same number of counts, yet there persists a definite deviation in the background behaviour. Note the excellent agreement in the peak profiles of the two patterns at D/Pd=0.72, yet the background profile is markedly different. Consider the two features in the D/Pd = 0.78 pattern (green line, medium dashes) marked with arrows. At points there is a pronounced step in the background counts, caused by calibration errors in the MRPD instrument. These could not be corrected.

As shown in Chapter 4 though, lattice parameters were successfully refined from the collected pattern.

3.6 HIFAR HRPD October 2003

Palladium powder of mass 11.2128 g, supplied by Goodfellow Metals, was sealed in a 316 stainless steel pressure vessel with 1.0 mm thick walls. This same sample had been used previously by Wu *et al* (see [12] and references therein) in their low temperature studies of Pd-D, and by Pitt and Gray (see [13]) whose results prompted the current study. Prior to the experiment the sample was annealed at 500°C (the estimated recovery temperature of Pd) under vacuum for approximately 12 hours, then cooled ambiently to room temperature and then taken through three absorption/desorption cycles with deuterium. It was then annealed again under vacuum at 500°C for another 12 hours. This pre-treatment was to place the sample in a similar condition to that as when it was used by Pitt and Gray[13].

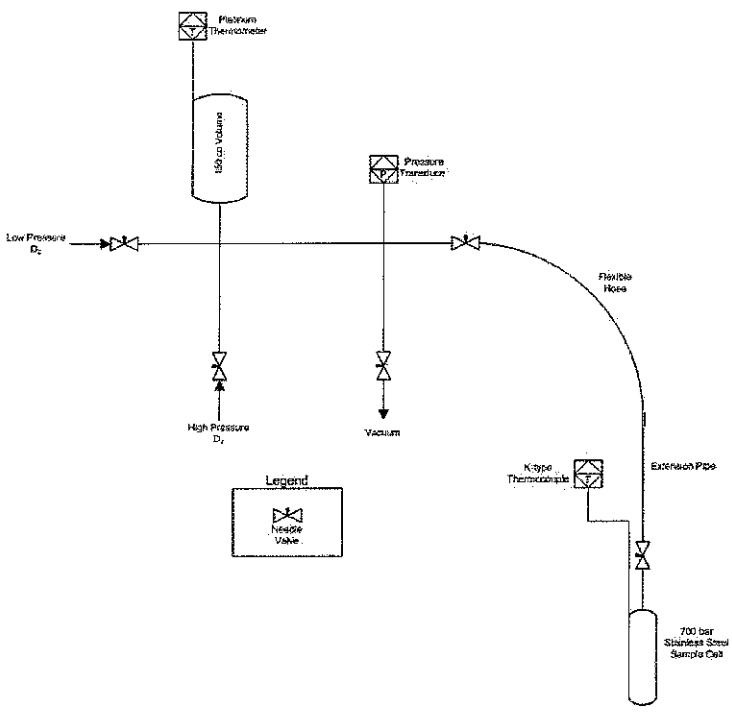

Fig 3.16 Schematic of Sieverts apparatus used on HIFAR HRPD October 2003

Neutron powder diffraction patterns were recorded using the high-resolution instrument HRPD at the HIFAR reactor at ANSTO, Sydney, in the 2θ range 0° to 150° in steps of 0.05°.

3.6.1 Manometrics

Fig 3.16 shows a schematic of the Sieverts apparatus used in this experiment. The total system volume was 252.9 cc

The p-c-T diagram obtained during the experiment is shown in Fig 3.17, and at each step a diffraction pattern was collected. The first three pressure steps were introduced at a temperature of 306°C after which the temperature was reduced to 301°C for the remaining steps up until the water quench step. For the quench the sample holder was removed from the furnace still at temperature and plunged into a bucket of water at ambient temperature. When the furnace had cooled to room temperature over a period of approximately 3 hours, the sample was placed back into the furnace to give the same background environment as before, and the room temperature pattern was collected.

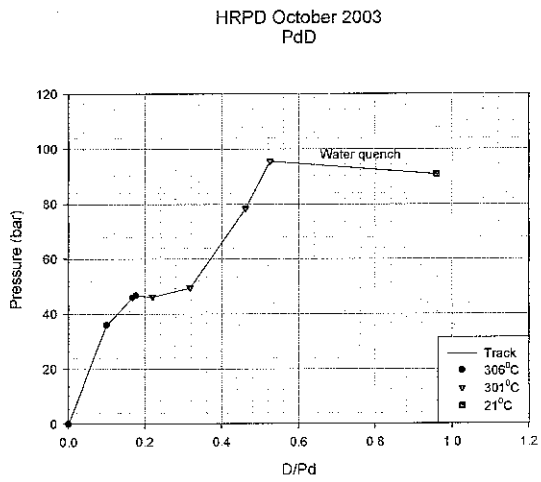

Fig 3.17. p-c-T diagram for palladium-deuterium, HIFAR HRPD October 2003

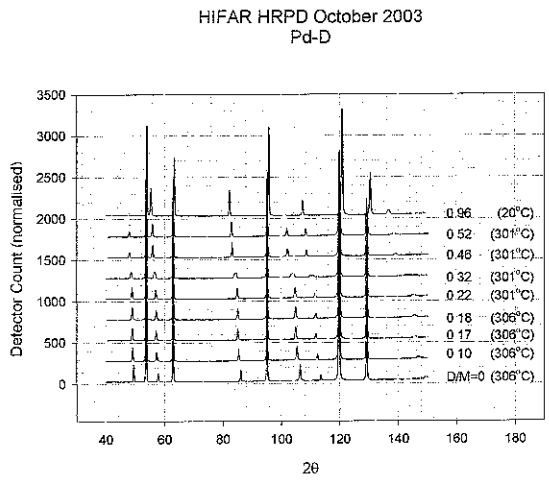

Fig 3.18 Diffraction patterns collected for palladium-deuterium on HIFAR HRPD October 2003

The deuterium-to-palladium atomic ratio of 0.96 achieved via the water-quench is quite remarkable. Pitt and Gray [13] calculated at maximum D/Pd of 0.78 using essentially the same technique with some minor differences. That study set the sample to 309°C and did not achieve as high a maximum pressure before the quench (69.33 bar compared to 95.50 bar in this study). Their quench was achieved by lowering the furnace temperature to 50°C by turning down its thermostat, and a pattern was collected at that temperature. The methodology used to calculate both numbers is identical and rigorous, and there is no reason at this point to doubt either of them. See chapters 4 and 5 for the results of the Rietveld analysis on the quenched-point pattern from the current study.

There was difficulty after the experiment in unloading the sample from its cell. The palladium powder had to some extent sintered and become a porous solid. This proved hard to dig out of the cell, as the process tended to compress the sample in the narrow confines of the cell-interior (internal diameter was 1 cm). The compression pushed the powder particles together into solid lumps if care was not taken and in the end only 11.187 gm were recovered (see Section 3.5)

3.7 ISIS HRPD March/April 2004

3.7.1 Issues Affecting the Proposed Beam-Time

The aim of this experiment was to repeat the experiment described in Section 3.4 on the more accurate High Resolution Powder Diffractometer (HRPD) at the ISIS neutron-beam facility at the Rutherford Appleton Laboratories (RAL) in Oxfordshire UK.

The recovered palladium from the experiment conducted in October 2003 (Section 3.5) was loaded into an identical sample cell as before. This experiment was originally scheduled to begin at the start of February 2004 on ISIS HRPD, and the sample and experimenters arrived at RAL late in January. Unfortunately, an electrical storm and blizzard the day before the start of our scheduled beam-time damaged the ISIS cyclotron. Its scheduled maintenance window was then brought forward, and as any repairs were slated to take approximately 10 days, our beam-time was cancelled. Thus our experiment was postponed until early May 2004. Before returning to Australia the pre-treatment as described in Section 3.4 was carried out and the sample was sealed under approximately 10 bar of deuterium, well into the beta-phase region at room temperatures, and left until our return 2 months later. Upon returning the pre-treatment was repeated, finishing with the sample under vacuum, before the experiment was loaded onto the HRPD instrument

Fig 3.19 shows a schematic of the Sieverts apparatus used in this experiment. The total system volume was 252.9 cc

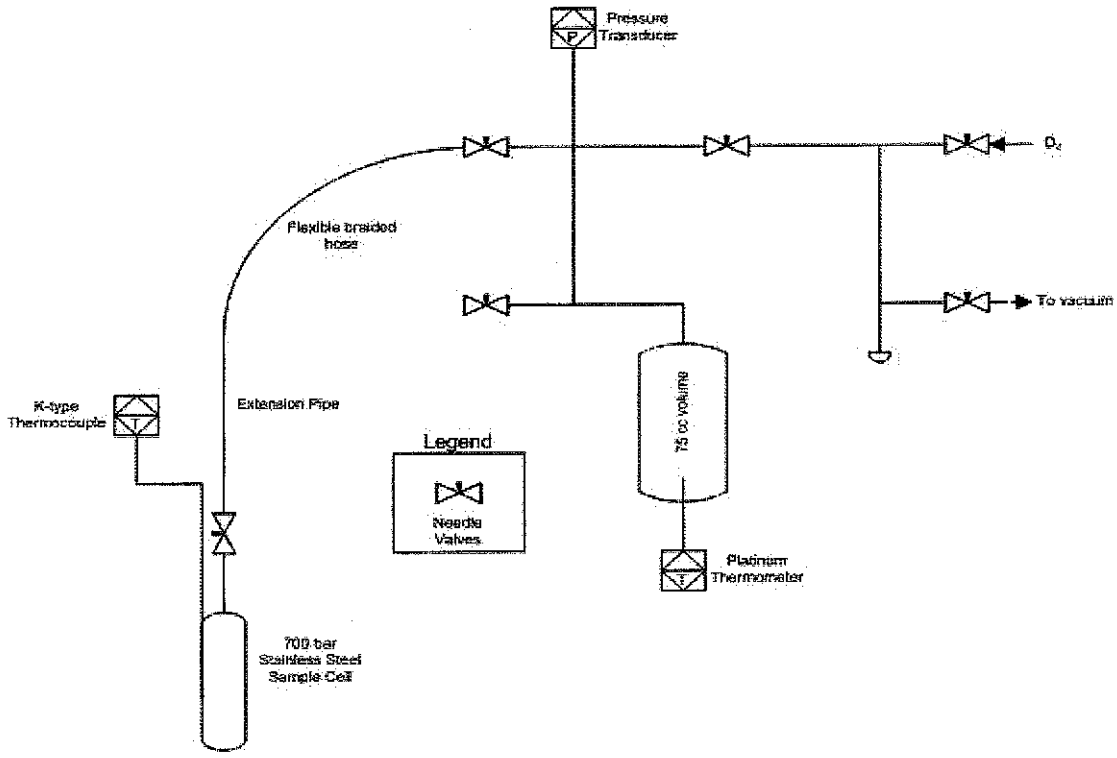

Fig. 3.19 Schematic diagram of Sieverts apparatus used on ISIS HRPD May 2004

3.7.2 Manometrics

Fig 3.20 shows the isotherms obtained during this experiment. The practice was to follow as closely as possible the manometry of Pitt and Gray [13] The experiment described in that paper showed evidence for tetrahedral occupancy of the FCC structure by the deuterium atoms. This was based on diffraction patterns taken on the HIFAR MRPD instrument, so it was hoped that the experiments described in this section, and the previous section, would confirm or deny these results by searching for the same phenomenon on the much higher resolution HRPD instruments at HIFAR and ISIS.

The series of pressure-temperature steps performed at ISIS follow, with reference to Fig 3.20:

After the initial pre-treatments described above, the sample was loaded into the RAL1 furnace on the HRPD instrument, and attached to the hydrogenator as shown in Fig 3.19. A diffraction pattern was the collected with the sample under vacuum at room temperature and

at 310°C. An absorption isotherm at 310°C was then followed (black upwards-pointing triangles) with patterns taken at a number of points. The desorption isotherm was then followed (empty downwards-pointing triangles), though only one diffraction-pattern was collected at 50.5 bar in order to confirm the existence of a two-phase point observed during the absorption isotherm. The desorption isotherm was halted at approximately 100 bar, and the sample was cooled to 120°C.

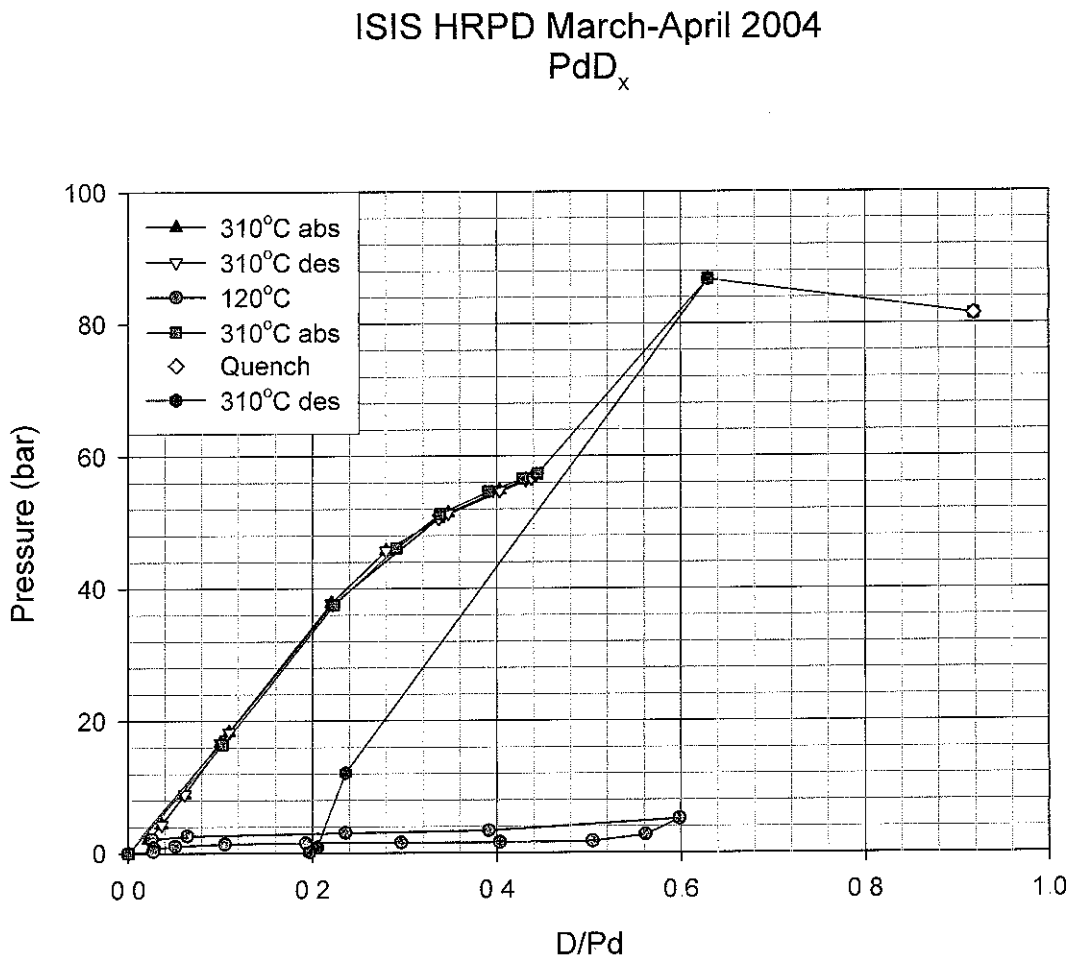

Fig 3.20. Pressure-composition-temperature graph of palladium-deuterium, obtained ISIS, RAL March-April 2004

An absorption and desorption isotherm was then followed at 120°C with patterns collected at several points. After confirming that the isotherm was returning to the origin i.e. the deuterium

was being completely removed, the sample was placed under vacuum. The temperature of the sample was then increased while still under vacuum, and patterns taken at temperatures of 310°C, 373°C, 436°C and 500°C to observe annealing effects (in Fig 3.20, all of these points are at the origin).

At this time, the sample was transferred under helium to a sample holder rated to higher pressure. This was to ensure that during the next isotherm (310°C) the final, highest point reached would be well above the two-phase region observed in the 310°C isotherm above. Upon placing the sample back on the HRPD instrument, the temperature of the sample was again taken to 310°C and a diffraction pattern collected. Then an absorption isotherm was again followed (green squares), though to a higher pressure than the previous. At a pressure of 87 bar (D/Pd = 0.63), a pattern was collected and the sample was quenched to room temperature by turning off the furnace and purging with helium (yellow diamond). Here diffraction patterns were collected for the remainder of the beam-time.

The sample and RAL1 furnace were then removed from the HRPD instrument, and the final desorption isotherm was followed (blue hexagons) without collecting any diffraction patterns to determine if any deuterium would remain trapped after the above steps, as reported by Pitt and Gray. It appears that approximately 0.2 D/Pd was trapped in the sample.

The diffraction run numbers, sample deuterium concentration and sample temperature are summarized in Table 3.1.

Fig 3.21 shows the results just described as plotted on the same set of axes as those of Wicke and Blaurock [1]. There is a marked difference in the shape of the isotherm obtained by Wicke and Blaurock at 310°C and the shape of the isotherms at 310°C obtained in this work. This difference agrees with the recent results of Tang *et al.* [14], who base their findings on both their own p-c-T diagrams and the published literature. They conclude that the thermodynamic properties of the palladium-hydrogen and palladium-deuterium systems depend upon the palladium morphology. Specifically that the α-phase hydrogen saturation solubility, and the adsorption plateau pressure, both increase with decreasing palladium particle size.

Table 3.1: ISIS HRPD April/May 2004 Manometrics

Run #	D/Pd (Manometric)	Temperature (°C)
R30176	0.0000	22
R30177	0.0000	310
R30178	0.1004	310
R30179	0.2206	310
R30180	0.2797	310
R30181	0.3475	310
R30182-30185	0.4376	310
R30186	0.3368	310
R30187	0.0259	120
R30188-30192	0.2359	120
R30193-30197	0.3915	120
R30198-30202	0.5985	120
R30203	0.0282	120
R30204-30209	0.0000	310
R30210-30215	0.0000	373
R30216-30220	0.0000	436
R30221-30226	0.0000	500
R30227	0.0000	310
R30228	0.3384	310
R30229-30234	0.4443	310
R30235-30238	0.6291	310
R30239-30241	0.9185	23

Wicke and Blaurock used palladium sheet to obtain their isotherms The α-phase saturation solubility can be estimated from Fig 3 21 as the approximate point where the slope of the isotherm begins to decrease as the isotherm approaches the "plateau". So, from Fig 3 21, visually estimating the α-phase saturation solubility for the 310°C isotherms gives $(D/Pd)_{sat}$~0 15 for sheet palladium, and (D/Pd)~0.25 for powder palladium. Similarly the inflexion point for sheet palladium is around 53 bar, and for powder palladium it is around 57 bar (this is confirmed in Chapter 4).

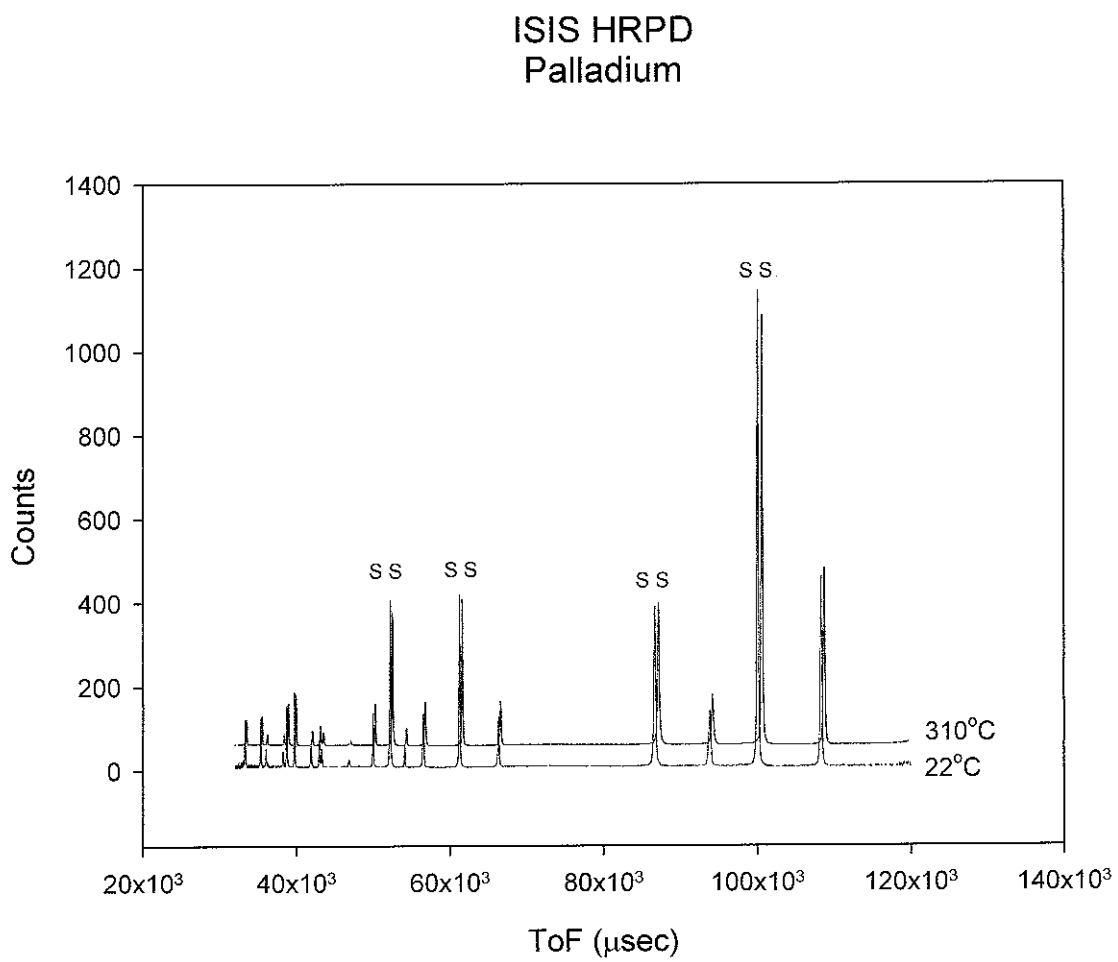

Fig 3 22 Neutron-beam diffraction patterns from palladium collected on ISIS HRPD instrument

Fig 3 22 shows the first two diffraction patterns taken of the sample, after the initial pre-treatment and before any exposure to deuterium. The patterns were taken with the sample at room temperature (22°C) and 310°C and nicely illustrate the effect of temperature on the diffraction pattern. All of the palladium and stainless steel diffraction peaks in the 22°C pattern are moved a uniform distance to the right, due to thermal expansion of the lattices, in the 310°C pattern.

Following is a more detailed look at each of the isotherms and their associated diffraction patterns (Fig's 3.23 to 3.30).

3.7.3 The Pre-dislocation 310°C Isotherm

Fig 3.23 shows the first absorption and desorption 310°C isotherm, with the patterns collected during this time shown in Fig 3 24. During the desorption steps (white down-pointing triangles) a concious effort was made to step to the same pressures visited during the absorption steps (red up-pointing triangles). The excellent agreement between the absorption and desorption points illustrates clearly the accuracy of the Sievert's technique and the manometric measurements, especially the

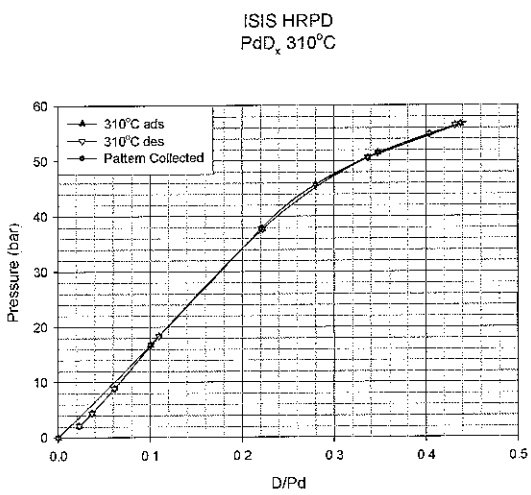

Fig 3 23 Palladium deuterium isotherm at 310°C

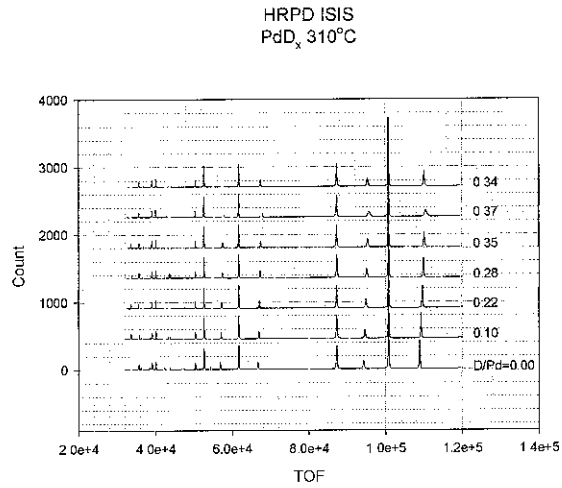

Fig 3 24 Palladium-deuterium neutron-beam diffraction patterns for 310°C isotherm collected HRPD ISIS

efficacy of the new deuterium equation developed for this thesis [15] (see Section 2.3.2) Note also the two-phase pattern apparent in Fig 3.24 at a deuterium to palladium concentration of 0.37.

3.7.4 The 120°C Isotherm

Fig 3.25 shows the absorption and desorption isotherm followed at 120°C, and Fig 3.26 represents the diffraction patterns collected at this temperature. The absorption leg of the 120°C isotherm is not as flat as would be expected, and the differences in the isotherms of this sample are clearly illustrated in Fig 3.21 Note that there is much better agreement between the desorption legs of the 120°C isotherms collected here and by Wicke and Blaurock [1] than there is in the absorption legs of same This could be due to a number of factors:

- Different sample types This work used a powdered sample, while Wicke and Blaurock used palladium sheet.
- The differing pre-treatments of the samples i e this works pre-treatments occurred immediately preceding traversal of a 310°C isotherm.

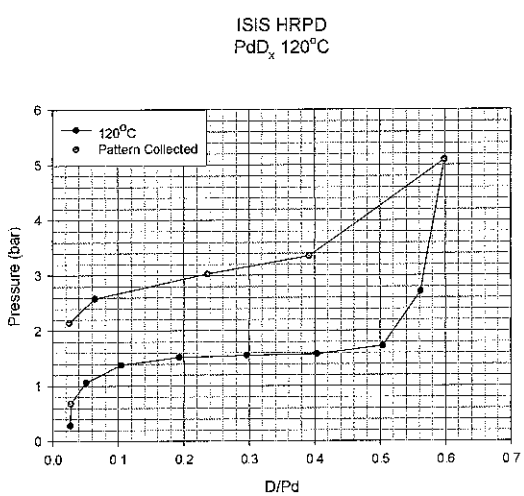

Fig 3.25 Palladium-deuterium isotherm at 120°C

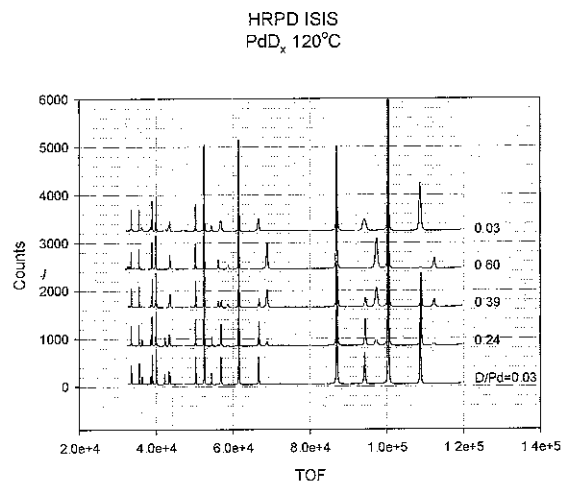

Fig 3.26 Palladium-deuterium neutron-beam diffraction patterns collected HRPD ISIS, sample at 120°C

- The history of the sample used here. This particular sample has been used in a number of hydriding and diffraction experiments over the last 15 years. This is the same sample as used in Section 3 4 above, and by Pitt and Gray [13]

- Wicke and Blaurock and Wu et al. [12] employed gravimetric methods to determine hydrogen-to-metal ratios, and used much smaller presure steps. It is possible that their measurements more accurately reflect equilibrium conditions

3.7.5 The Annealing Temperature Scans

Fig 3 27 shows the diffraction patterns collected during the temperature scan part of the experiment. Traversal of the sample through the two-phase part of the 120°C isotherm will introduce defects due to the co-existence of two phases with different lattice parameters and this should be apparent in patterns collected before and after the 120°C isotherm. 500°C is thought to be above the palladium annealing temperature, so a diffraction pattern was collected at a few temperatures as the dislocated sample was heated under vacuum from 310°C to 500°C. Fig 3.28 shown detail of the [111] and [200] peaks shown in Fig 3.27.

It is clear from both Figures 3.27 and 3.28 that cycling the sample through the two-phase region at 120°C has introduced significant peak broadening caused by micro-strain dislocations (see bottom two patterns in both figures). Note that there is more broadening in the 310°C pattern than in the pre-cycled 120°C pattern, but the 310°C pattern has less broadening than the post-cycled 120°C pattern. This means that significant annealing is already taking place at 310°C

The post-annealed 310°C pattern exibits far less peak-broadening than the pre-annealed 310°C pattern, illustrating that 500°C is sufficiently high for the annealing process

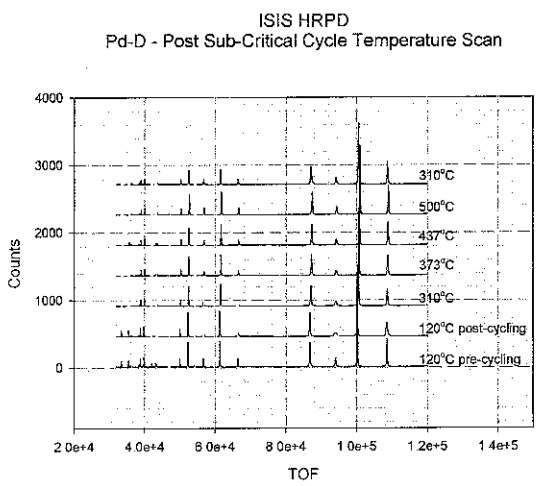

Fig 3.27 Palladium annealing temperature neutron-beam diffraction patterns HRPD ISIS

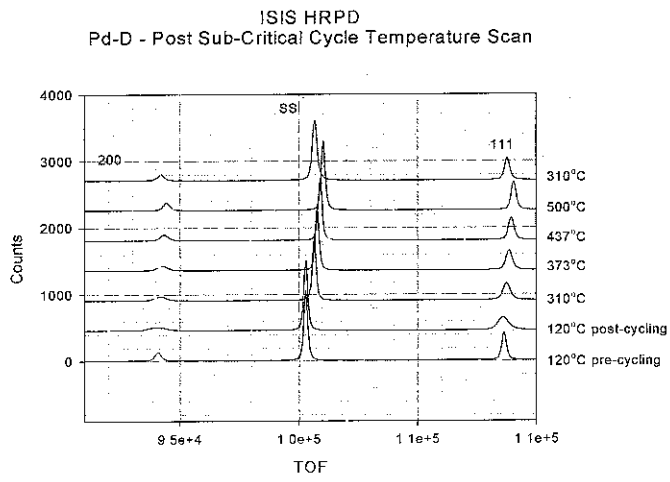

Fig 3.28 Palladium annealing temperature neutron-beam diffraction patterns HRPD ISIS (detail)

3.7.6 The Post-Annealing 310°C Isotherm and Quench

Fig 3.29 details the final 310°C isotherm, the quench step to room-temperature, and the desorption isotherm showing the final trapped deuterium. Fig 3.30 shows the diffraction patterns collected during this stage, all coming from the absorption isotherm except for the final pattern taken from the quenched sample.

It can be seen from Fig 3.21, that the post-annealing 310°C isotherm follows the track of the initial 310°C isotherm. So, as far as the manometrics are concerned, the annealing has returned the sample to a state near to its condition at the start of the experiment.

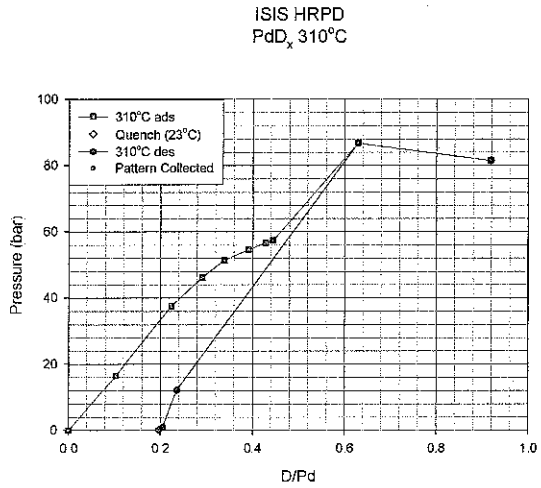

Fig 3.29 Palladium-deuterium 310°C isotherm and quench step

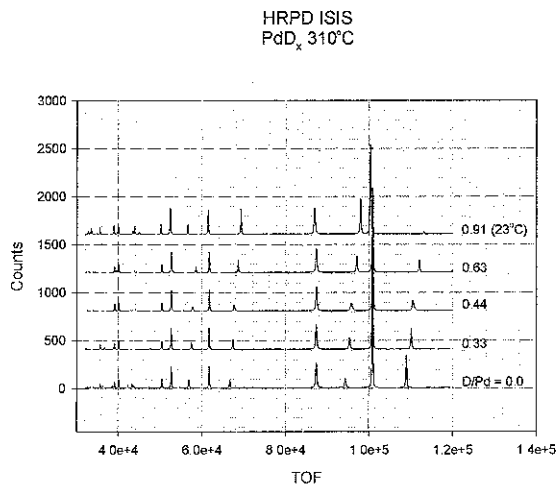

Fig 3.30 Palladium-deuterium neutron-beam diffraction patterns collected HRPD ISIS

As with the quench performed at ANSTO in October 2003 (Section 3.4) a significant amount of deuterium was absorbed in the quench performed here. At ANSTO, the quench was performed by plunging the sample cell into a bucket of water, dropping the temperature from 310°C to room temperature in a matter of seconds, achieving a maximum deuterium to metal ration of 0.96. At ISIS the furnace was turned off and flushed with He gas, dropping the temperature of the sample from 310°C to 28°C over about 100 min and only achieving a deuterium to palladium ratio of 0.92. The quench performed by Pitt and Gray [13] was obtained by turning off the furnace, and cooling the sample for approximately 4 hours. The maximum concentration achieved in this process was approximately 0.78. It appears from these results that increasing the rate of temperature decrease will increase the total deuterium trapped in the quenched sample.

3.8 Conclusions and Discussion

The critical temperature of a palladium-hydrogen system can be determined by observation of the disappearance of either one of two forms of measured hysteresis within the system. The first indirect method is the hysteresis that occurs between the absorption-leg and desorption-leg of the palladium-deuterium p-c-T diagram. The second direct method, fully explored in Chapter 4, involves the disappearance of two distinguishably different palladium-deuterium phases (α and β) via measurement of their associated lattice parameters. The two-phases can be observed by eye in many of the patterns listed above, but the true behaviour of the phases can only be fully understood via their Rietveld analysis.

The p-c-T isotherms presented in the current chapter present evidence that the critical temperature of palladium-deuterium varies according to the form of the bulk palladium, solid sheet or powdered. The series of isotherms presented from the experiments performed in October 2001 on MRPD at ANSTO (Figs 3.2, 3.4 and 3.6) agree closest with Wicke and Blaurock [1], assuming that the isotherm at 280°C did in fact clip the peak of the two-phase region.

The experiments of October 2003 and March/April 2004 on the powdered palladium sample, where an obvious two-phase pattern was observed at 301°C and 310°C respectively, reveals two things:

1. The critical temperature of palladium-deuterium depends on the physical bulk form of the sample, and
2. p-c-T diagrams are not accurate enough to allow determination of the exact thermodynamic critical temperature, regardless of whether gravimetric or manometric techniques are used to determine deuterium concentrations

Wicke (in [16], but quoting results from [17-20]) states that there are observable differences between the p-c-T two-phase isotherms of bulk palladium and palladium black. The desorption isotherm plateau pressures and the critical points (T_c, P_c, n_c) of the two forms agree within error. Palladium black isotherms compared to bulk palladium have smaller hysteresis loops and are shifted towards higher H/Pd concentration values.

The narrower loops are attributed to the nucleation of the β-phase being facilitated by the highly defective lattice of the palladium black. Less mechanical stress is accumulated in the crystals of the palladium black, compared to bulk palladium, as the phase transition proceeds from the surface to the bulk. The shift of the isotherms to higher H/Pd values is due to chemisorption of hydrogen at the surface of the sample, which is complete (one hydrogen atom per surface palladium atom) at low hydrogen pressure before the dissociated hydrogen can diffuse into the bulk.

The first 310°C isotherm from March/April 2004 (section 3.7.3) displays no sign of hysteresis between the absorption and desorption legs, and no sign of a plateau region. According to popular convention, this would indicate that the 310°C isotherm lies entirely above the critical point, yet it is obvious from the diffraction patterns collected that a two-phase region was traversed. This means that 310°C is below the critical temperature. This result is explored further in Chapter 4, with some discussion of the nature of the two distinguishable phases.

The results of Chapter 3 also illustrate the accuracy of the new deuterium compressibility equation developed by the author [15]. All of the isotherms presented that traversed both absorption and desorption legs returned accurately to the zero position, a sure indication of the equation's accuracy, especially considering some of the large pressure steps performed. This is especially apparent in the isotherm of Fig. 3.23, where the desorption leg accurately follows the path of the absorption leg.

Any errors in the calculation of deuterium compressibility would accumulate during both the absorption and desorption stages, leading to the isotherm not returning to zero. The nature of these errors is such that as zero pressure is approached, a non-zero deuterium concentration would result, which in the past has led to experimenters assuming small amounts of trapped deuterium in samples after completion of isotherms. This is entirely different to the large amount of deuterium trapped after the quench step of section 3.5.6. Chapter 4 contains a discussion on the nature and cause of this trapping.

1. Wicke, E and J. Blaurock, *New Experiments on and Interpretations of Hysteresis Effects of Pd-D_2 and Pd-H_2.* Jounal of the Less-Common Metals, 1987 **130**: p. 351-363
2. Feenstra, F. and R. Griesen, *Electronic density-of-states from pressure-compsition isotherms in metalhydrides* Solid State Communications, 1986 **59**(12): p. 905-908
3. Davis, W D., *Knolls Atomic Power Laboratory Report Number 1375*, in *Knolls Atomic Power Laboratory Reports* 1955, Knolls Atomic Power Laboratory.
4. Worsham Jr , J.E., M.K. Wilkinson, and C.G. Shull, *Neutron-Diffraction Observations on the Palladim-Hydrogen and Palladium-Deuterium Systems.* J. Phys. Chem. Solids, 1957. **3**: p. 303-310
5. Lewis, F A., *The Palladium/Hydrogen System.* 1967, London: Academic Press Inc. 178
6. Amandussen, H , L.-G. Ekedahl, and H. Dannetun, *The effect of CO and O_2 on hydrogen permeation through a palladium membrane* Applied Surface Science, 2000. **153**: p. 259-267
7. Wang, D., T.B. Flanagan, and K.L. Shanahan, *Permeation of hydrogen through pre-oxidised Pd membranes in the presence and absence of CO.* Journal of Alloys and Compounds, 2004. **372**: p. 158-164.
8. Ali, J.K., E.J. Newson, and D.W.T. Rippin, *Deactivation and regeneration of Pd-Ag membranes for dehydrogenation reactions.* Jounal of Membrane Science, 1994. **89**: p. 171-184
9. Morreale, D.D , et al., *Effect of hydrogen-sulphide on the hydrogen permeance of palladium-copper alloys at elevated temperatures* Jounal of Membrane Science, 2004. **241**: p. 219-224
10. Roa, F. and J.D. Way, *The effect of air exposure on palladium-copper composite membranes.* Applied Surface Science, 2005 **240**: p. 85-104.
11. Fukai, Y , *The Metal-Hydrogen System.* Springer Series in MaterialsScience, ed. H.K. Lotsch. Vol. 21. 1993, Berlin: Springer-Verlag. 353.
12. Wu, E., et al , *The Ordered Structure of $PdD_{0.78}$ at 70-75K* J. PHys. Condens. Matter., 1996 **8**: p. 2807.
13. Pitt, M.P. and E.M. Gray, *Tetrahedral Occupancy in the Pd-D System Observed by In Situ Neutron Powder Diffraction.* Europhysics Letters, 2003. **64**(3): p. 344-350.
14. Tang, T., S.-l. Guo, and G.-d. Lu, *Relationship between Palladium Morphology and Thermodynamics in Palladium-Hydrogen System.* Materials Science Forum, 2005 **275-279**: p. 2485-2488
15. McLennan, K.G. and E.M. Gray, *An equation of state for deuterium gas to 1000 bar.* Measurement Science and Technology, 2004. **15**: p. 211-215.
16. Wicke, E. and H. Brodowsky, *Hydrogen in Palladium and Palladium Alloys*, in *Hydrogen in Metals II: Appication-Orientated Properties*, G. Alenfeld and J. Volkl, Editors. 1978, Springer-Verlag: Berlin. p. 73-155.
17. Frieske, H. 1972: Munster.
18. Frieske, H. and E. Wicke, Ber. Bunsenges. Physik. Chem., 1973 **77**: p. 50
19. Nernst, G.H. 1963: Munster.
20. Wicke, E. and G.H. Nernst, Ber. Bunsenges. Physik. Chem., 1964. **68**: p. 224.

Chapter Four

In-situ Neutron-beam Diffraction Studies of the Palladium-Deuterium System:

Lattice Parameters

Chapter Four

In-situ Neutron-beam Diffraction Studies of the Palladium-Deuterium System:

Lattice Parameters

4.1 Introduction

Lattice parameter data is one of the least ambiguous pieces of information that can be obtained using Rietveld analysis of diffraction patterns, coming directly from Bragg's Law,

$$2d \sin\theta = n\lambda , \tag{4.1}$$

where d is the spacing of the crystal lattice planes, and λ is the wavelength of radiation used. Only small doubt of the exact position of the peaks can occur due to thermal motion peak-broadening and instrumental peak-broadening.

The earliest reported x-ray studies of hydrided solid palladium [1-3] miss much of the detail now apparent in the hydrogen-palladium lattice parameters, and show a discontinuous lattice parameter, an indication of co-existing phases. These phases have been confirmed as the low concentration solid solution and the high concentration palladium-hydride. The palladium lattice parameter appeared to jump from the α-phase value of $a = 3.89$ Å to the β-phases value of $a = 4.02$ Å at a hydrogen to palladium concentration H/Pd of ~0.1, and then remained constant with increasing hydrogen concentration until the maximum concentration of H/Pd ~0.6 was reached. Many subsequent studies of the 1920s and 1930s performed below the thermodynamic critical temperature [4], confirm these findings.

Some evidence for a gradual increase in lattice parameter with increasing hydrogen concentration was also presented, but modern studies [9] still quote the discontinuous results. The current study, with its use of modern high-resolution neutron-beam diffactometers, shows that both scenarios (linear versus discontinuous) can be obtained, depending on the exact conditions under which the palladium is hydrided, and how much care is taken with sample preparation and in determining hydrogen to palladium concentrations. This is most evident in the studies that isolated the hydrided specimens from oxidizing atmospheres during the X-ray measurements and measured the amount of hydrogen out-gassed under vacuum later. Studies that failed to do this may have lost hydrogen from samples spontaneously during X-ray exposure.

The single-phase nature of palladium-hydrogen above the thermodynamic critical point was demonstrated by the first modern experiment using *in-situ* X-ray diffraction [6].

The claim of a discontinuous lattice parameter (room temperature α-phase lattice parameter of 3.89 Å and a room temperature β-phase lattice parameter of 4.02 Å) has been repeated regularly in the intervening years, including in [10] quoting X-ray investigations, and as recently as 1990 in [11] via an *in-situ* neutron diffraction study of electrochemically loaded palladium-deuterium.

In the current study the hydrogenation/dehydrogenation (deuteration) of the samples were performed from the gaseous phases *in-situ* on the neutron diffraction instruments. Great care was taken to ensure that palladium and deuterium were not exposed to oxidizing atmospheres at anytime during cycling.

In an early application of x-ray diffraction to the analysis of crystal structure, Vegard [12, 13] observed that in many ionic salt alloys a linear relation held, at constant temperature, between the crystal lattice constant and relative concentration of the constituent elements. This empirical rule has since become known as *Vegard's Law*. Subsequent extensions of this law to metallic alloys show that the majority of systems do not to obey it. The current neutron-beam diffraction studies however show that single-phase regions of the palladium-hydrogen (or at least the palladium-deuterium) system *do* obey Vegard's Law. The two-phase regions, at sub-critical temperatures, obey a form of Vegard's Law.

All lattice parameters in this chapter were determined via Rietveld analysis using the Australian Rietica Windows based profile analysis code [15] (see Section 4.2)

For the pure phase samples, the lattice parameters follow Vegard's Law. This lattice expansion results from the addition of the hydrogen's electrons to the palladium band structure. Since at D/Pd = 0.63 (at temperature 0K) the d band of the palladium is supposedly filled, it can be expected that the slope of Vegard's law may change at this point (see results here in Section 4.5).

The structure of pure palladium has been confirmed in numerous diffraction studies and is known to be face-centered cubic (FCC). The highest symmetry possible for this structure is the space group *Fm3m*, which is therefore the easiest one to use for any refinements. It is known that the metal atoms do not move from this structure during absorption of hydrogen or deuterium. The positions in the face centered cube that the hydrogen atoms will occupy are the octahedral and tetrahedral positions. At stoichiometric PdH (or PdD) where H/Pd=1, assuming the hydrogen atoms occupy the octahedral position of the face-centered palladium structure, the structure of the hydride will be the simple-cubic structure of NaCl. This has been confirmed in [10, 14]

4.2 Rietveld Analysis

For all patterns collected both α-phase and β-phase were modeled using space-group *Fm3m*. Sample and instrument issues prevented full analysis of the data collected in October 2001 and July 2002 (see Sections 4.3.2 and 4.4.2 for details), though lattice parameter data was obtained from all.

The general methodology for refining the palladium-deuterium patterns was consistent throughout the experiments. This involved estimating thermal parameters initially based on previous neutron-beam diffraction studies in the literature, then refining the major variables (background, lattice parameters, phase scales, occupation numbers) one at a time until a reasonable fit was obtained. At this point the thermal parameters are refined and if reasonable values obtained, the whole process is repeated until the best fit possible is obtained.

The methodology used to determine the tetrahedral and octahedral occupations in Chapter 5 was slightly more complicated and is detailed in that chapter.

4.3 HIFAR MRPD October 2001

4.3.1 Introduction

Details of this experiment including sample characteristics, experimental setup and the HIFAR Medium Resolution Powder Diffractometer are described in Chapter 2 and Section 3.3

4.3.2 Refinement problems

The sample used in this experiment was a palladium sheet rolled into a cigar-shape (i.e. a spiral) before placement in the sample cell. Cold rolling of the sample during manufacture introduces preferred orientation and it was hoped that the spiral would average these effects. This was not the case, and preferred orientation in the sample meant that the diffraction data could not be fully analysed. The preferred orientation model in the Rietica program was not sophisticated enough to account for all of the texture present in the sample.

It was possible to extract excellent lattice parameter data from the diffraction patterns, which are presented below. All refinements were modeled with only octahedral deuterium occupation of the palladium FCC lattice allowed (see Chapter 5 for why this is important). For an explanation of the special positions in the FCC lattice, see section 6.2.1 of Chapter 6.

4.3.3 The Super-Critical Isotherm

The refined lattice parameters of the supercritical isotherm (300°C), shown in Fig 4.1, follow Vegard's law. The lattice parameters show a direct linear increase with increasing deuterium concentration. As there is no hysteresis present in a supercritical isotherm, the desorption isotherm patterns were not recorded.

Error bars in the refined lattice parameter are included in Fig 4 1 and a linear fit of the data, calculated using a least-squares algorithm, has been plotted to show the excellent agreement with Vegard's Law The errors on the lattice parameters increase with increasing deuterium concentration As an octahedral-occupation-only model was constrained on the system the errors may be due to the existence of tetrahedral site occupation at these higher deuterium concentrations (see Chapter 5).

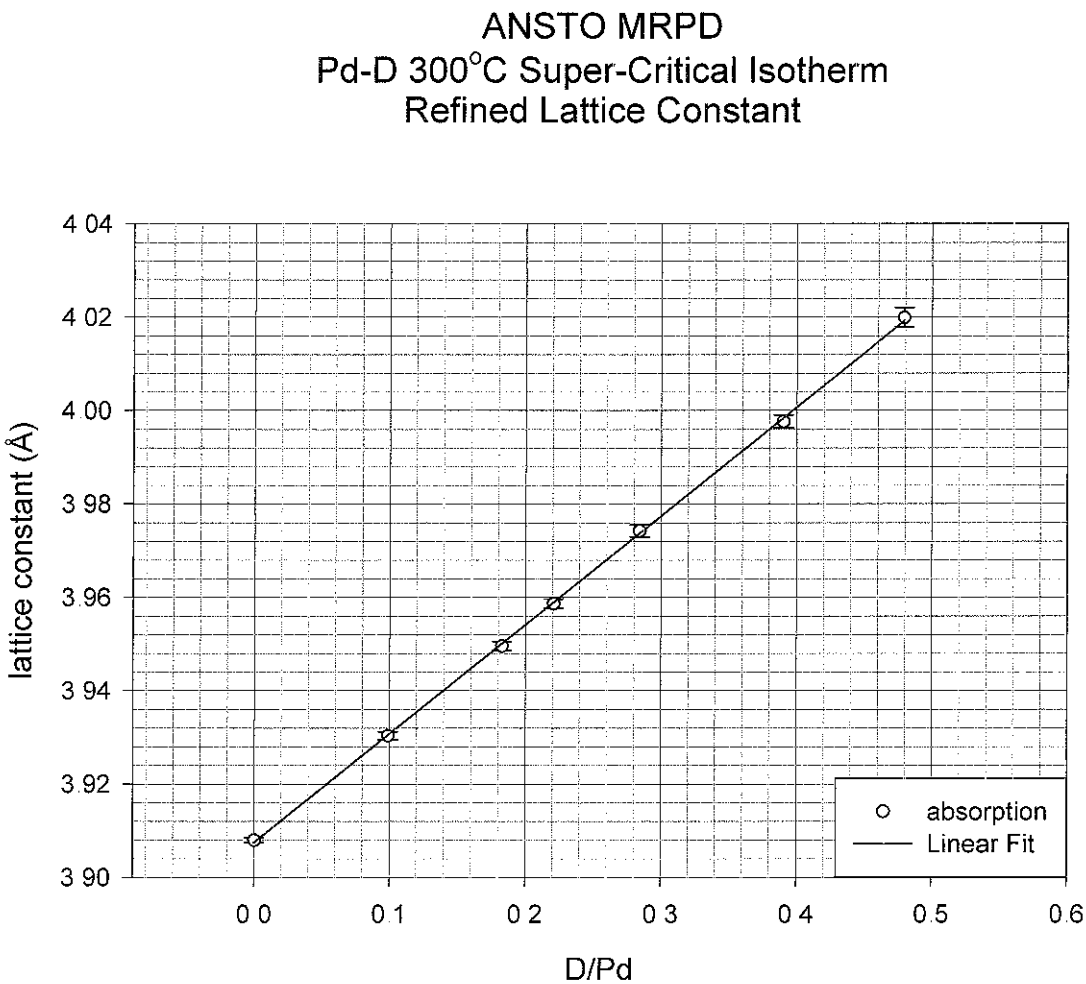

Fig 4 1: Supercritical isotherm (300°C). Refined lattice parameter versus deuterium content, absorption isotherm only

4.3.4 The Critical Isotherm

The lattice parameters refined from the critical-temperature isotherm (280°C) are shown in Fig 4.2. That is a straight line with slight splitting due to the presence of alpha and beta phases that are very similar (see confirming results in Section 4.6 describing an ISIS HRPD experiment performed in May 2004). The resolution of MRPD is not enough to determine if the temperature used was slightly above the critical temperature, though the discrepancies between the absorption parameters and the desorption parameters which are not consistent, suggests that some inhomogeneity may be occurring in the sample. The texture of the rolled palladium sheet used for the sample ensured that other parameters in the refinement, which

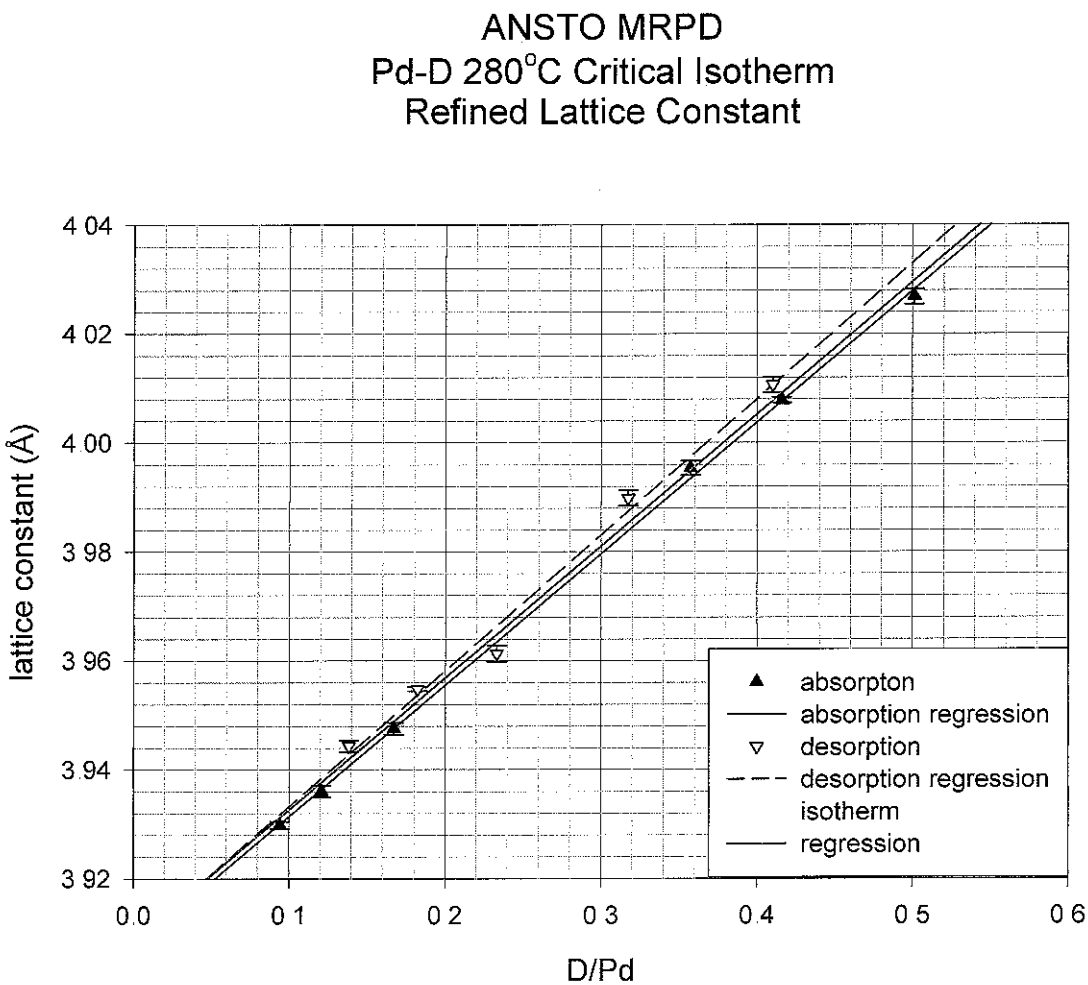

Fig 4.2: Critical isotherm (280°C). Refined lattice parameter versus deuterium content, absorption and desorption isotherms. Solid black line is a linear regression through the absorption points, dashed black line is a linear regression through the desorption points, solid red line is a linear regression through all points

may have confirmed a two-phase structure, could not be refined

Three linear regressions have been calculated for the data in Fig 4.2 The solid black line uses the absorption data only The dashed black line uses the desorption data only. The solid red line is fitted to all the data. The errors on the lattice parameters have a tendency to increase with the increasing deuterium concentration, and as with the critical isotherm, this may be an indication of occupation of the tetrahedral FCC cell sites by deuterium atoms.

4.3.5 The Sub-Critical Isotherm

250°C was selected as a suitable temperature to investigate the two-phase region of the peri-critical region of the palladium-deuterium system. The refined lattice parameters plotted against the deuterium content of the sample is shown in Fig. 4.3

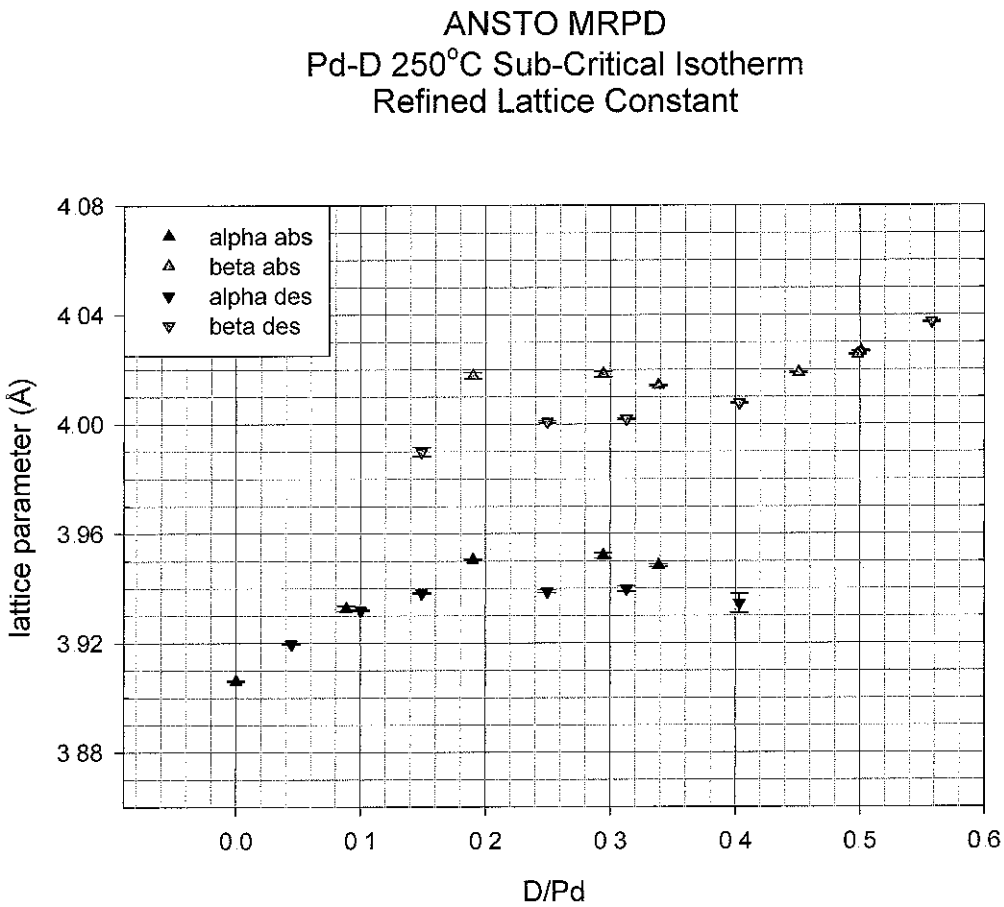

Fig 4.3: Sub-critical isotherm (250°C). Refined lattice parameter versus deuterium content, absorption and desorption isotherms

The point of interest here is the different lattice parameters obtained for alpha and beta phases. Initially during the formation of the dilute solid solution phase, the lattice parameter of the α-phase follows Vegard's law as with the super-critical sample Eventually the β-phase begins to nucleate at approximately D/Pd = 0.1 at which concentration the α-phase lattice parameter is approximately 3.95 Å. This is followed by appearance of beta phase lattice parameter reaching a maximum of approx 4.02 Å, while the alpha phase lattice parameter stays constant. There is an increasing amount of beta phase until D/Pd=0.4, the point at which a super-critical single-phase sample would reach a lattice parameter of 4.02 Å, at which point the whole system is beta phase. Then there is a gradual expansion of the beta phase lattice parameter following Vegard's Law again

There is hysteresis apparent in both the α-phase lattice parameter and in the β-lattice parameter between absorption and desorption. There is over-heating in the α-phase and β-phase lattice parameter in that both plateau lattice parameters decrease slightly with increasing deuterium concentration There is under-cooling evident in the α-phase during desorption as the α-phase plateau lattice parameter increases slightly with decreasing deuterium concentration.

Note that the relative error of each lattice point increases as the relative amount of each phase decreases in the two-phase region i e alpha phase decreases with increasing deuterium concentration and beta phase decreases with decreasing deuterium concentration.

4.3.6 The Peri-Critical Region Lattice Parameters

Fig 4 4 shows the refined lattice parameters from the supercritical, critical and sub-critical isotherms above plotted on the same axes Note here that the 250°C two-phase data shows a symmetric splitting around the linear Vegard's Law section obeyed by the single-phase data.

4.4 SINQ HRPT May 2002

4.4.1 Introduction

Details of this experiment including sample characteristics, experimental setup and the SINQ High Resolution Powder Diffractometer - thermal neutrons are described in Chapter 2 and Chapter 3. Insurmountable problems with the manometrics of this experiment meant that that data had to be abandoned. It was possible to extract the lattice parameter data successfully, using the deuterium-to-palladium ratios calculated from the Rietveld refinement of the collected patterns.

4.4.2 Lattice Parameters

Fig 4.5 shows the lattice parameters refined from the collected diffraction patterns. As with the refinements from HIFAR MRPD from October 2001 described in section 4.3, the lattice parameters follow a form of Vegard's Law. There is a linear relationship between lattice-parameter and deuterium-to-palladium concentration for the single-phase data. The two-phase lattice-parameters at D/Pd = 0.27 sit on either side of the single-phase line.

These results call into doubt the critical temperature of palladium-deuterium. The two-phase pattern was collected during the first isotherm at 295°C. This is well above the critical temperature of Wicke and Blaurock [16], which is the value assumed and confirmed in section 4.3 (compare the results of Fig 4.5 with those of Fig 4.2.)

4.5 HIFAR HRPD July 2002

4.5.1 Introduction

Details of this experiment including sample characteristics, experimental setup and the HIFAR Medium Resolution Powder Diffractometer are described in Chapter 2 and Chapter 3.

4.5.2 Refinement Problems

Problems arising from the incorrect calibration of the MRPD instrument have already been discussed in section 3.5.2. These issues ensued that only lattice parameter data could be refined from the collected diffraction patterns.

4.5.3 Lattice Parameters

Fig 4.6 shows the lattice parameters refined from the collected diffraction patterns

The point to note from these results is that the rate of increase of the lattice parameter decreases at the highest concentration values (this is more apparent in Fig 4.7) , due to the donated electrons from the deuterium having filled the palladium d-band at D/Pd ~ 0.6. From here the donated electrons are likely filling the Palladium 5p and 6s bands. This indicates that the addition of deuterium does not expand the lattice as much as at lower deuterium concentrations. These are conditions that could facilitate cold fusion, where it is conceivable that if the trend continues as the deuterium concentration increases then additional deuterium atoms could be packed close enough to other deuterium atoms to fuse.

At this time, the only previous diffraction studies to examine palladium-hydrogen at these concentrations are those of [5, 7]. See Fig 4.21 for a comparison of these results and others.

This effect is more readily apparent when these results from July 2002 are compared with the lattice parameters refined from the experiment of October 2001 detailed in Section 4.2. This comparison is shown in Fig 4.7

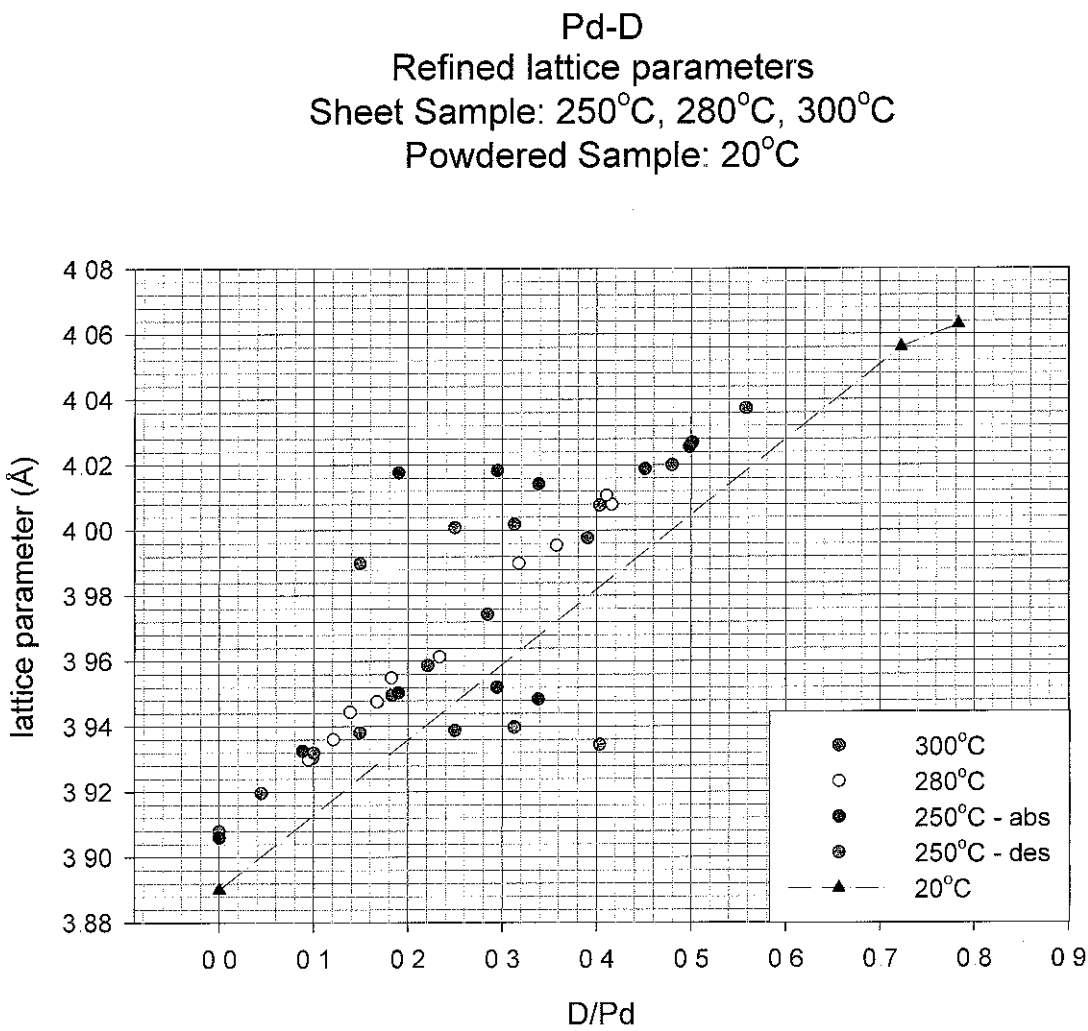

Fig 4.7 Comparison of lattice parameters refined from experiments of October 2001 and July 2002

The room temperature data of July 2002 follows the same form of Vegard's Law as the peri-critical temperature data of October 2001, though offset by an amount due to the thermally induced lattice expansion of the higher temperature sample.

4.6 HIFAR HRPD October 2003

The details of the manometry measurements for this experiment are detailed in section 3.5 This comprised the start of a 306°C adsorption isotherm changed to a 301°C isotherm before the critical point At the top of the isotherm the sample was water-quenched to room temperature

Fig 4.8 plots the refined lattice parameters obtained from all diffraction patterns collected in October 2003 The sample at D/Pd concentrations of 0.22 and 0.32 was two-phase. The change in temperature from 306°C to 301°C was done at D/Pd = 0.18 before stepping to D/Pd = 0.22

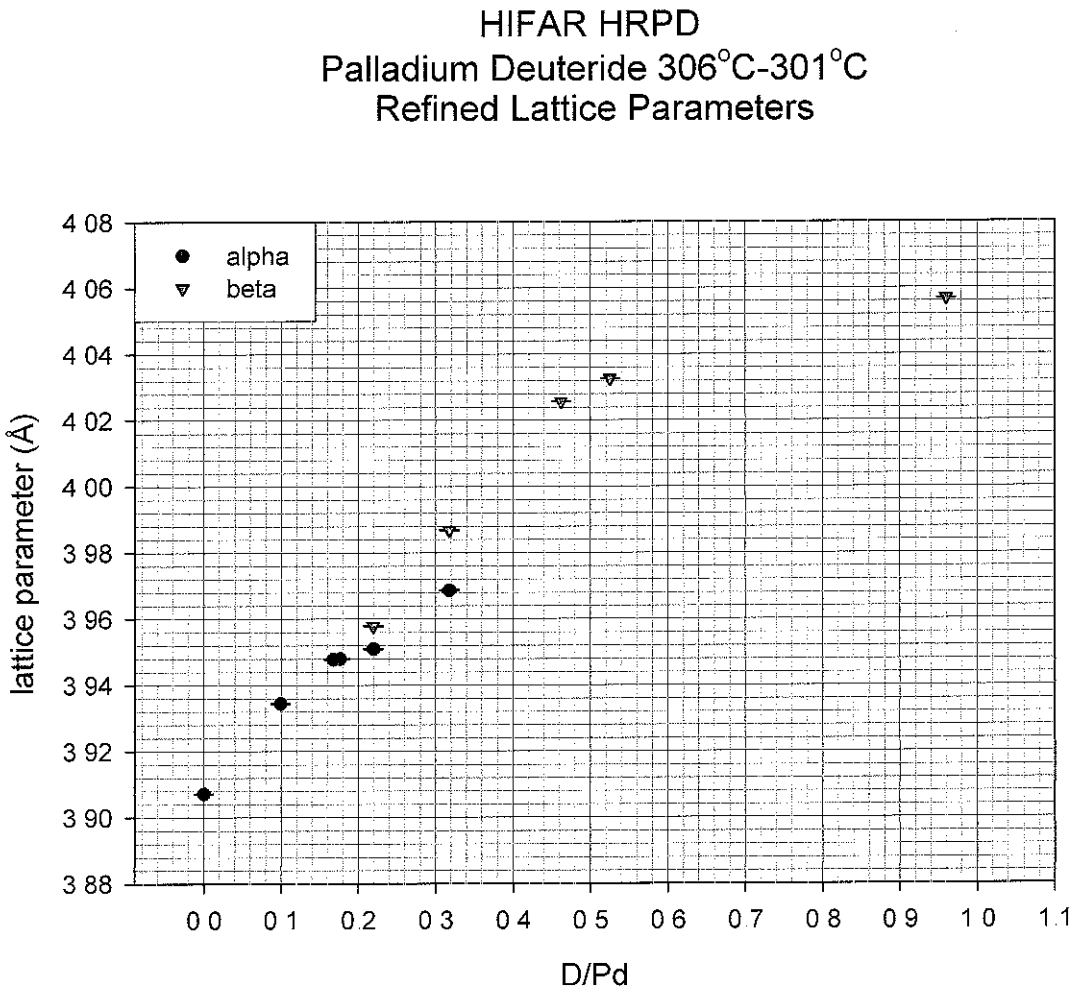

Fig 4.8 Refined lattice parameters of palladium-deuterium on HRPD HIFAR October 2003

In Fig 4 8 it appears as if the 2-phase beta lattice-parameters and pure-phase beta lattice-parameters are an extension of the pure-phase alpha parameters, but this is due to the change in temperature at D/Pd=0 18. Although the 2-phase alpha lattice parameters appear shifted from the main line, the lattice parameters of the two phases are in fact exhibiting a weak splitting as hinted at in the 280°C isotherm of Section 4 3.4 This weak splitting is also shown in the results from the experiment performed in March/April 2004 at ISIS RAL (see Section 4 7 2.)

The α-phase and β-phase lattice parameters from the two-phase region of these results do not stay constant as the typical two-phase lattice parameters refined at temperatures well below the critical temperature (see section 4 3.5). Instead, when this close to the critical temperature, the two phases are similar enough that there is not enough induced strain between them to cause dislocations and allow nucleation of one phase in the other. Instead they behave like two super-critical phases existing together, each separately following Vegard's Law.

4.7 ISIS HRPD March/April 2004

4.7.1 Introduction

As detailed in Section 3.7.2, the temperature/pressure steps followed in this experiment can be grouped into the following areas of interest, during each of which neutron-beam diffraction patterns were collected at thermodynamically interesting points

1 The first 310°C isotherm (adsorption and desorption)

2 The120°C isotherm (adsorption and desorption)

3 The annealing temperature scan

4. The second 310°C isotherm (adsorption and desorption)

5. The quench to room temperature

4.7.2 The Lattice Parameters of the Pre-Dislocation 310°C Isotherm

Figure 4.9 shows the refined lattice parameters from the initial 310°C isotherm followed. The very first diffraction pattern, collected before heating the sample to 310°C is also shown. It was the two-phase pattern observed at the highest pressure reached in Fig 4.9 that prompted transfer of the sample to a higher-pressure-rated sample -cell for the second 310°C sample.

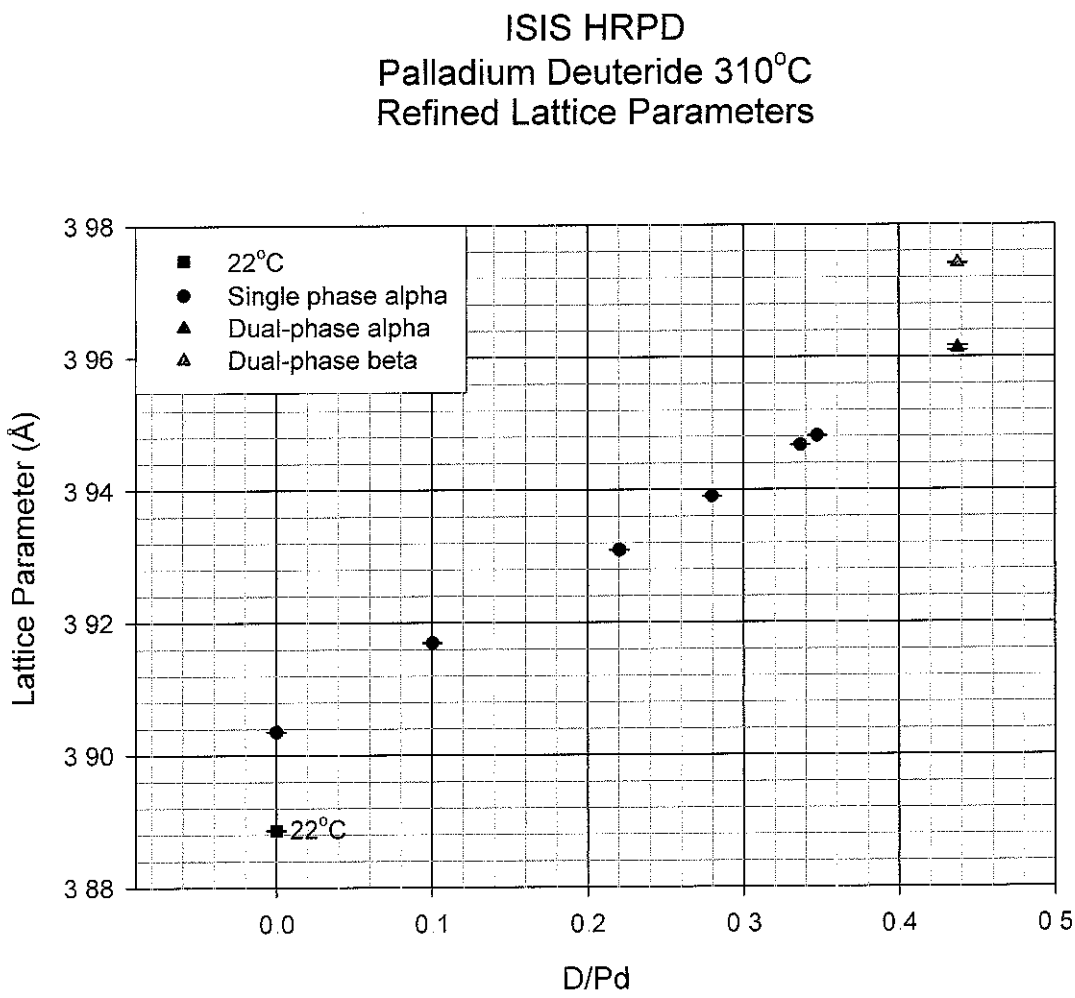

Fig 4.9 Refined palladium-deuterium lattice parameters for 310°C isotherm

The existence of distinguishably different lattice parameters for two phases separately obeying Vegard's Law at a temperature of 583 K places the critical temperature for this sample

significantly higher than previously determined. Wicke and Blaurock [16] determined T_c=556 ± 1 K for palladium-deuterium, while Fukai [17] publishes 536 ± 1 K based upon the disappearance of hysteresis in the pressure-composition isotherms. The results of analysis in Section 4.4 involving data from the lower resolution MRPD agree with these lower values. Lewis [18] reports T_c = 295.3°C (568.5 K), and 295°C is often assumed in the literature.

Wicke and Blaurock [16] calculated a critical concentration n_c=0.257±0.0004 for both PdH and PdD. This is not unreasonable, considering the sparseness of the data in the two-phase region in Figure 4.8 (which shows the same sample under very similar conditions), that the beta-phase will disappear around n = 0.2 - 0.3. When considered separately the single phase lattice parameters both follow the same form of Vegard's law, but transposed along the *a*-axis. The interaction between deuterium atoms in the palladium matrix is causing this.

4.7.3 The Lattice Parameters of the 120°C Isotherm

The sub-critical 120°C isotherm lattice parameters collected at ISIS, shown in Fig 4.10, are very similar to those collected at ANSTO in October 2001 at 250°C. The alpha- and beta-phase lattice parameters appear constant over the range of concentrations and pressures investigated here. The overall relationship to Vegard's Law becomes apparent when the 120°C data are plotted on the same axes as the data collected at 310°C (Section 4.7.2), as shown in Fig 4.11.

Given the apparent discontinuous change in lattice parameters from alpha- to beta-phase, it would be interesting to see how the lattice parameters evolve around the splitting points (alpha to mixed alpha/beta points and beta to mixed alpha/beta point) by utilizing small, very accurate pressure steps. As this could prove time consuming due to the large number of addition patterns to be collected, it might best be studied using synchrotron radiation.

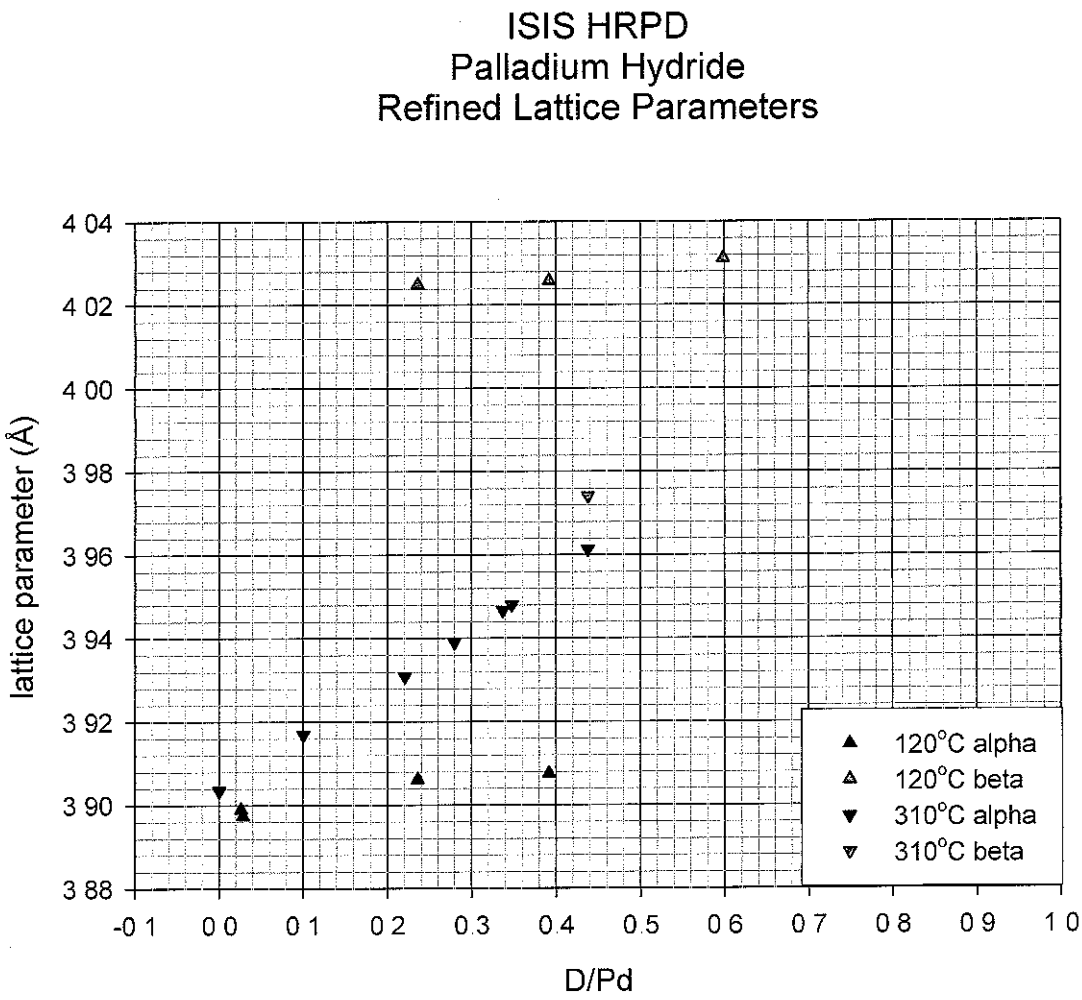

Fig 4 11 Critical and sub-critical lattice parameters

4.7.4 The Annealing Temperature Scan Patterns

After the 120°C isotherm was completed, the sample cell was evacuated and the sample left under vacuum. The temperature of the sample was then raised to 310°C, 373°C, 437°C, and 500°C and a one-hour diffraction pattern was collected at each temperature. Rietveld analysis of these patterns revealed worthwhile data illuminating some of the annealing processes in the palladium crystal structure. Firstly, Fig 4.12 shows the increase in the FCC lattice parameter with the increasing temperatures

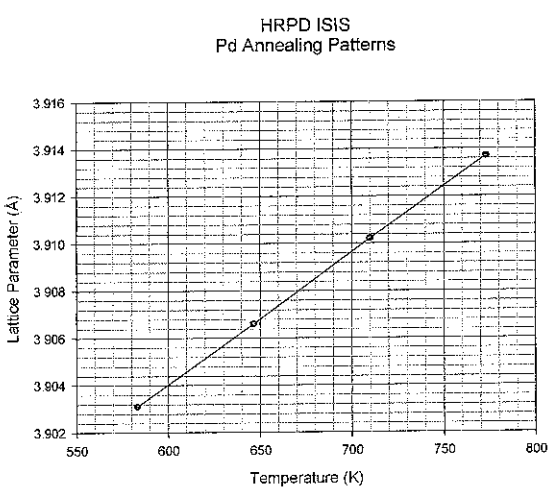

Fig 4.12 Annealing temperature patterns

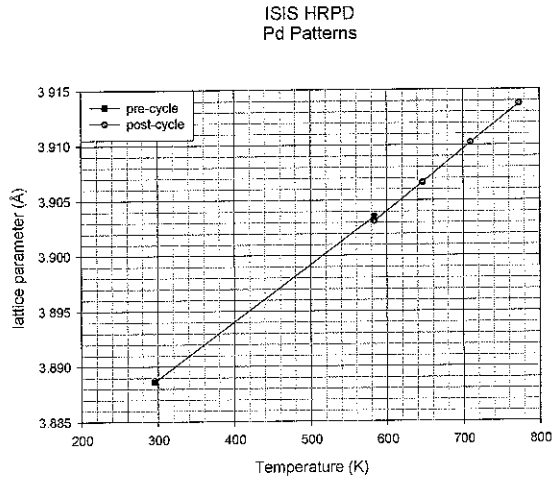

Fig 4.13 All pure palladium lattice parameters

Fig 4.13 shows the points from Fig 4.12, along with the lattice parameters refined from the first two diffraction patterns collected at ISIS, on the un-deuterided palladium, taken at room temperature and 310°C. The slight discrepancy in the two lattice parameters refined at 310°C is due to error in the set temperature of the RAL1 furnace. Between these two patterns the temperature of the furnace, initially at 310°C was lowered to 120°C and increased back to 310°C as the first annealing run temperature. The sample temperature then did not return to the exact temperature as before (or at least the same average temperature over the length of time taken to collect a pattern) and the high resolution of the HRPD instrument was able to resolve this difference via the thermal expansion of the palladium lattice. This is good evidence then not only for the excellent accuracy of the ISIS HRPD instrument, but also for the temperature stability of the RAL1 furnace.

The difference between the two refined 310°C lattice parameters (3.9035 Å and 3.9031 Å) is 0.0004 Å. Given the rate of linear thermal expansion of palladium is 11.8×10^{-6} K^{-1} at 0°C and assuming the same value at 310°C this indicates an actual temperature difference at the sample close to 0.1°C.

Fig 4.14 through 4.17 shows the changes in some of the parameters affecting peak-shape with the increasing temperatures of this stage of the experiment. The actual refined numbers, including lattice parameter, are shown in Table 4.1

Table 4.1

Temperature (°C)	a (Å)	B (Å^2)	γ_1 (Å^{-1})	γ_2 (Å^{-2})	A_{size} (Å)
310	3.9031	0.5116	154.6510	-80.7130	84.9029
373	3.9066	0.6619	116.9550	-67.3010	71.1524
437	3.9102	0.8315	92.0980	-53.0540	67.1300
500	3.9137	0.9549	60.0040	-46.1340	68.1830

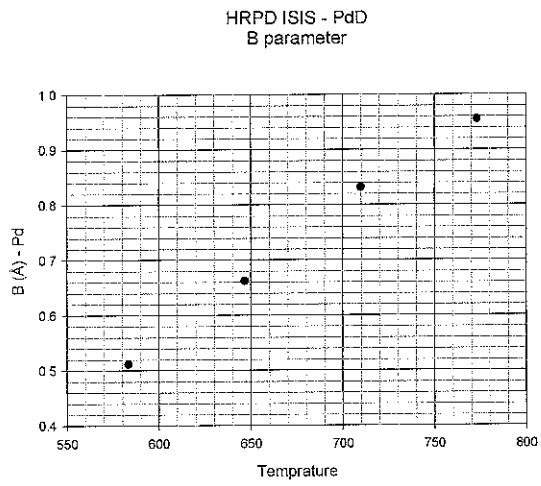

Fig 4.14 Refined thermal parameter B during annealing

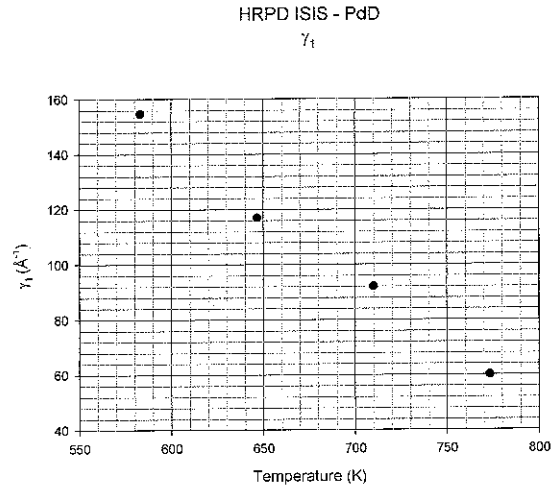

Fig 4.15 Refined peak-shape parameter γ_1 during annealing

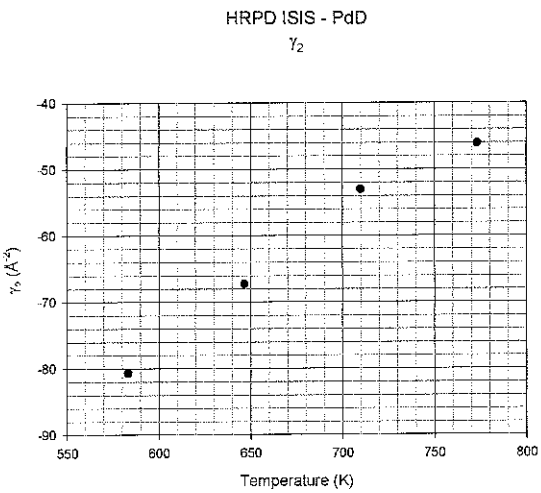

Fig 4.16 Refined peak-shape parameter γ_2 during annealing

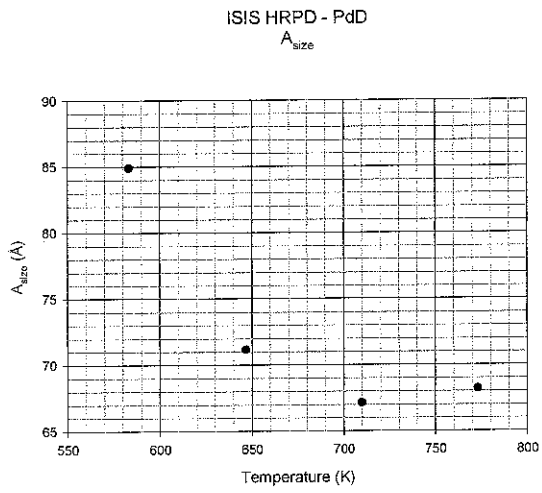

Fig 4.17 Refined particle-size parameter A_{size} during annealing

In order to illustrate the relative behaviour of the four peak shape parameters, Fig 4.18 shows these peak-shape parameters normalized to their maximum value over the range of temperatures, and plotted on the same axes. These maximums were B(T=773K), γ_1(T=583K), γ_2(T=583K), A_{size}(T=583K)

There is a steady increase in thermal parameter with temperature consistent with increasing thermal motion of the palladium atoms with increasing temperature. The particle size parameter, A_{size} decreases steadily till approximately 700K, and then becomes constant. This parameter is *inversely* proportional to actual particle mosaic size. The particle size is increasing until the dislocations induced during passage of the sample through the two-phase region during the 120°C isotherm are annealed out, and the original particle size of the sample is recovered.

There is a steady decrease in both γ_1 and γ_2 with increasing temperature. These are both peak broadening terms, which indicates a reduction in the strain fields induced in the sample during passage through the two-phase region.

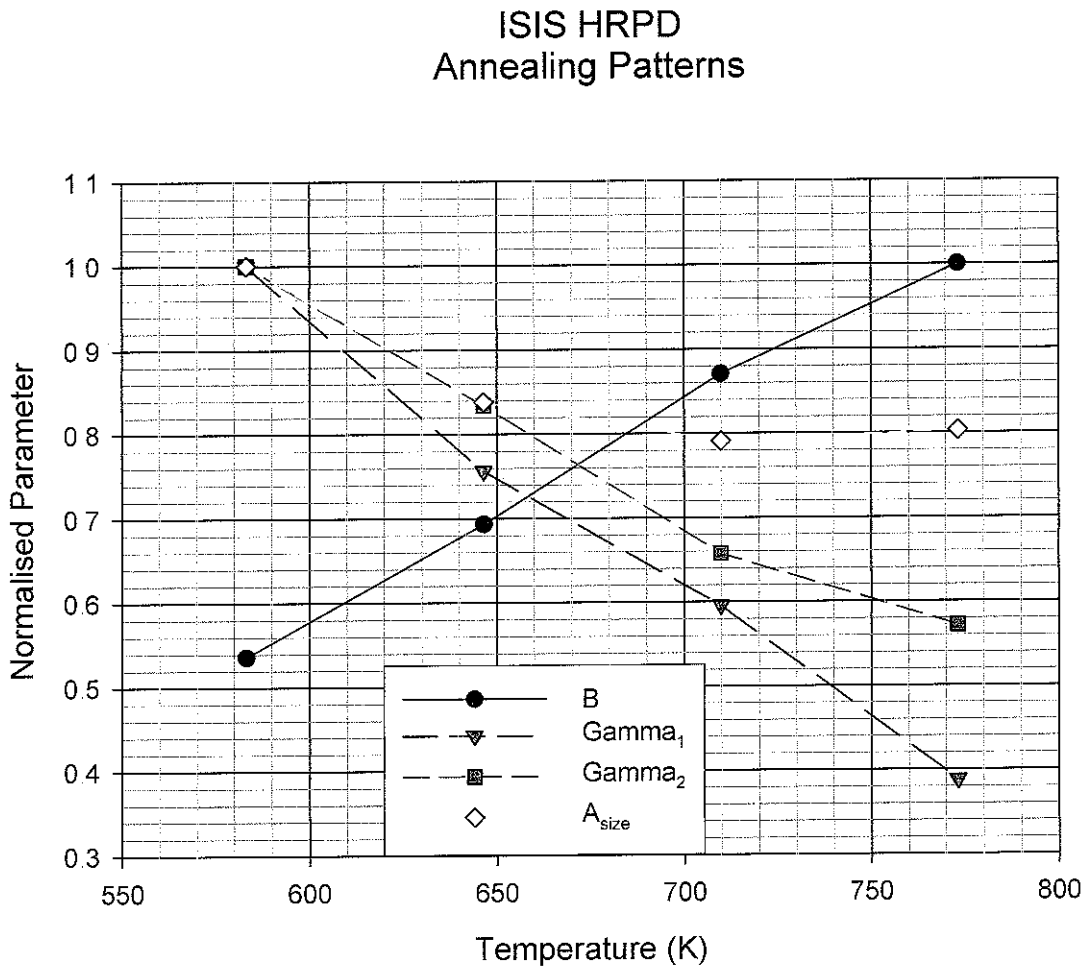

Fig 4.18 Palladium-deuterium annealing experiment peak-shape parameters

Passage of the sample through the two-phase region at 120°C increases the density of dislocations in the sample, therefore increasing elastic strain. This is evident in the increased peak broadening in the diffraction patterns taken immediately after the 120°C isotherms. Under annealing, the peak broadening terms do not return to their original value until the annealing temperature has reached 500°C, though they have begun to recover at the lower temperatures. To ensure the removal of the background dislocation density we have shown that annealing at 500°C for several hours is necessary.

4.7.5 The Post-Annealing Lattice Parameters

The patterns collected after the annealing experiment are four patterns collected during the absorption leg of the second 310°C isotherm along with the pattern collected from the quenched sample.

Fig 4.19 shows the lattice parameters that were refined from three patterns collected during the adsorption leg of the second 310°C isotherm, prior to the quench, along with those of the quenched sample. As before, the alpha phase lattice parameters follow Vegard's Law.

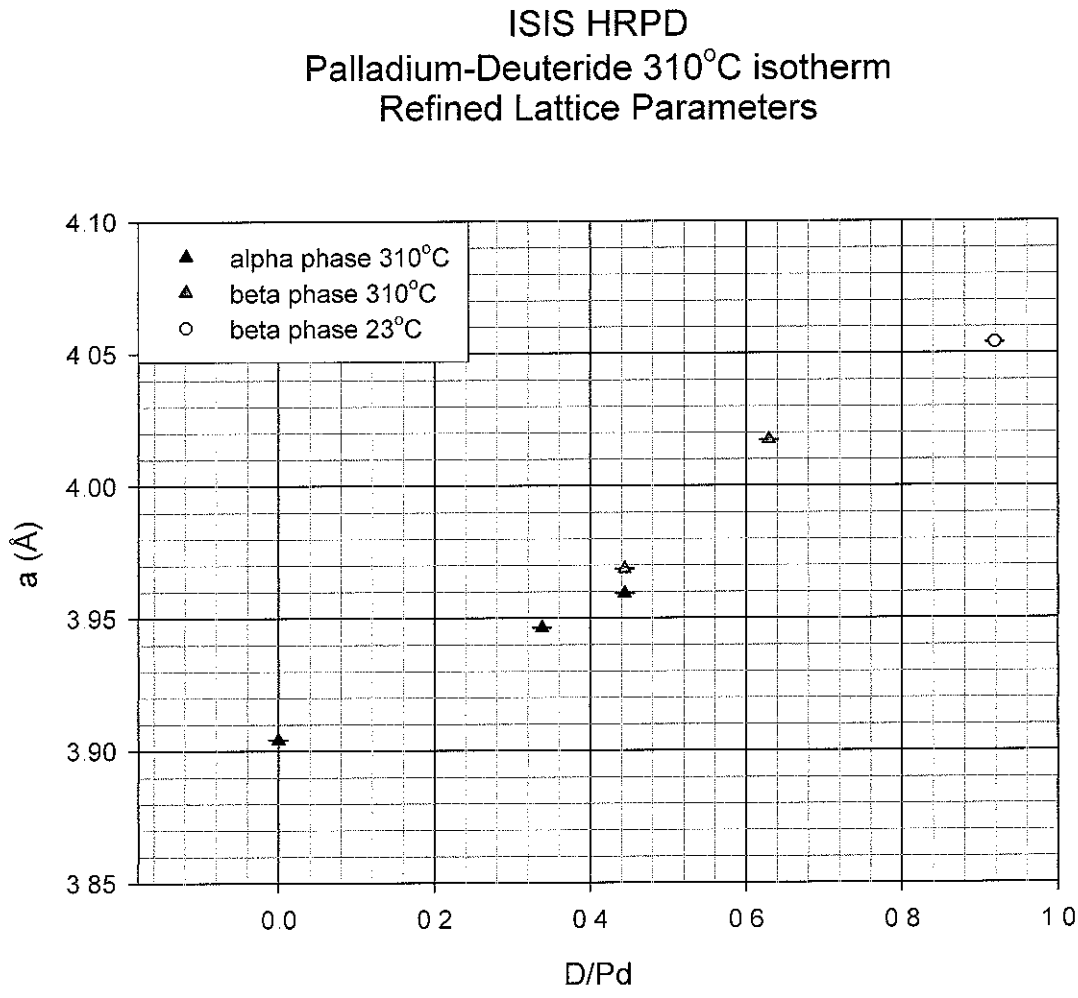

Fig 4.19 Lattice parameters of the palladium-deuterium 310°C isotherm and quench

4.7.6 All ISIS HRPD Results

It is worth here displaying all the results collected during March-April 2004 on HRPD at ISIS, RAL. This is done in Fig 4.20. As with the results from October 2001 (section 4.4.2), the lattice parameters here all follow the same form of Vegard's Law. Any single-phase lattice parameters follow the classic form of Vegard's Law, while the two-phase lattice parameters are symmetric about the single-phase line.

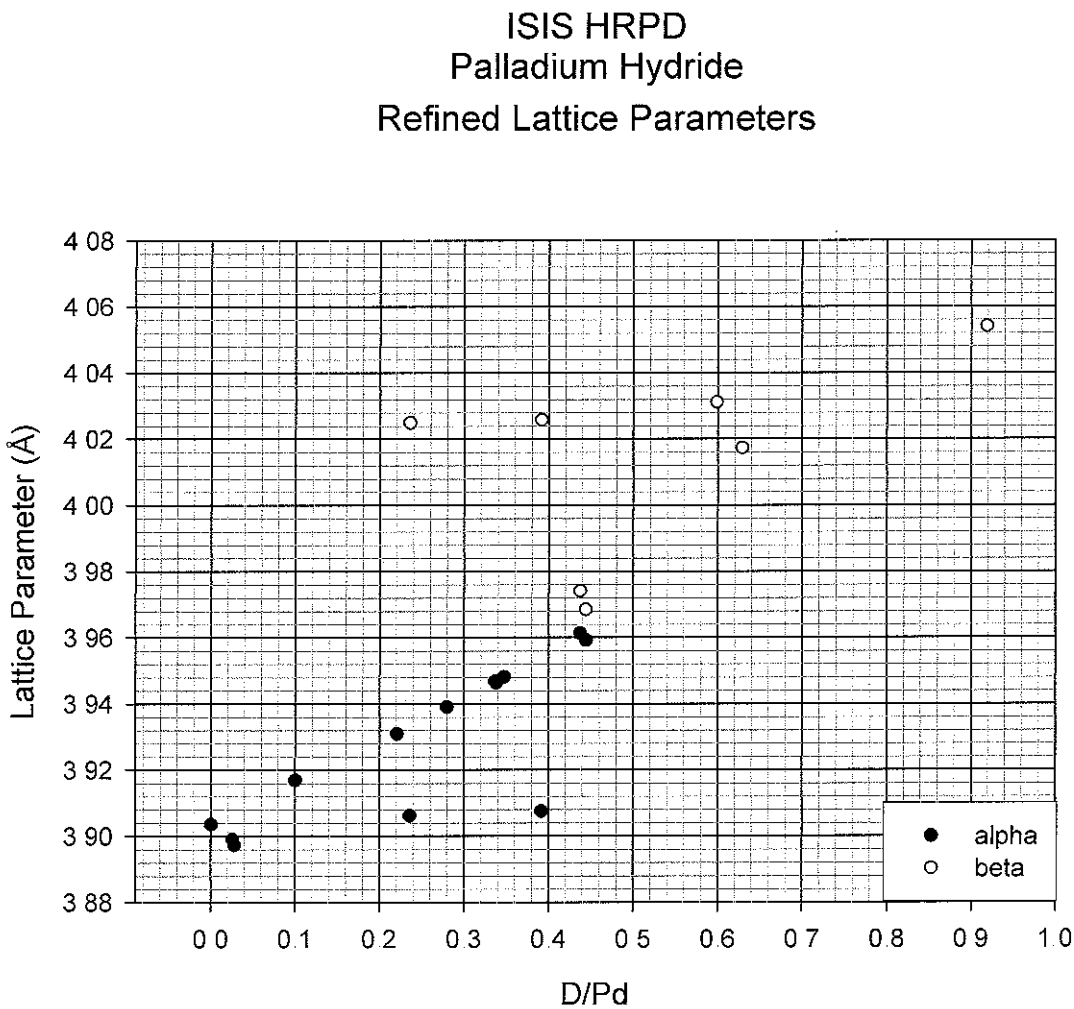

Fig 4.20 All results from ISIS HRPD March/April 2004

4.8 Comparison of All Results

Fig 4.21 shows all the results collected so far from the current research for temperatures near the critical temperature, along with results from previous studies. All results shown follow the same form of Vegard's Law, with slight differences in the slope of the relationship. Baronowski's results exhibit a similar change in slope of the concentration-lattice parameter curve as was found in the current experiment of July 2002. Remember that for the experiments of this thesis dated 2003 and 2004 the highest D/Pd point of both was a quenched sample.

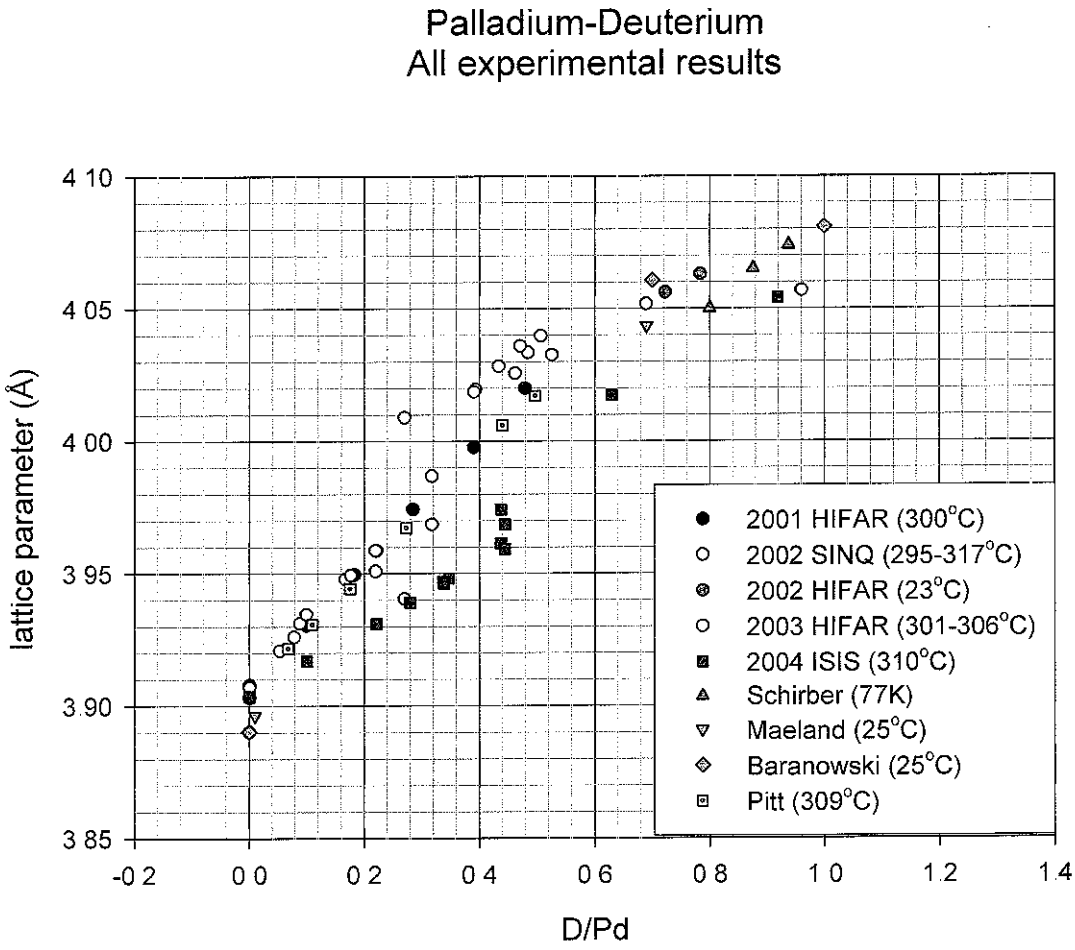

Fig 4.21: The lattice parameters of PdH_x and PdD_x from neutron-beam diffraction studies. Results are from experiments reported in this thesis (dated results) and from [5-8]

Note that it is apparent that the general slope of the lattice parameter/concentration relationship changes at D/Pd ~ 0.6, the concentration where the palladium "4d" band supposedly fills. From this point the extra absorbed deuterium are contributing electrons to the "5s" band, thus the change in slope.

The result from the quenched sample from October 2003 stands out as an anomaly when held up against all the results of Fig 4.21. This phenomenon is thought to be a result of an effect proposed by Erich Kisi of the University of Newcastle [19]. Due to the quenching, a contraction of the lattice parameters from the drop in sample temperature combined with slower diffusion kinetics and a sudden absorption of deuterium due to passage along the system isochore, results in a condition exhibiting a higher than equilibrium deuterium concentration. Very slow kinetics of desorption from this position occurs, resulting in apparent "trapped" deuterium when the system pressure is reduced to near vacuum. This "trapping" was apparent in the October 2003 experiment, but those measurements are not shown in Section 3.6 (see Fig 3.17). The trapping is shown quite clearly in the experiment of April 2004 at ISIS RAL (Section 3.6 and 3.7, see specifically Fig 3.18). It is important to note that this trapping occurred even though the desorption of the deuterium was performed after returning the sample temperature to 310°C.

4.9 Conclusions and Discussion

We have performed a neutron-beam diffraction study of the lattice parameters of the palladium-hydrogen system about the critical temperature. We have shown that Vegard's Law is obeyed by individual phases with two-phase patterns symmetric about the single-phase line. The expansion of the lattice under Vegard's Law is an electronic effect.

The slope of Vegard's Law can be influenced by the amount of contamination of the palladium sample. Oxides of palladium may not be in sufficient quantities to show up as separate phases, but will have electronic effects that may change the slope of Vegard's relationship. Two of the experiments shown in this chapter display lattice parameter results that deviate from those of the other studies by following different slopes in Vegards Law i.e. those of 2002 SINQ HRPT and 2004 ISIS HRPD.

The sample used at SINQ was of unknown history, and had a very dull, grey appearance. It is thought that the surface of this sample was very heavily oxidized. The sample from ISIS does have a known history and it is a long and chequered one. Over the last 20 years this palladium sample has been used in numerous hydriding experiments and has spent literally months illuminated by neutrons. It is also likely that it contains impurities. The necessity to leave the sample in England during the period our beam-time was postponed may have contributed to contamination.

We have shown that the critical temperature of palladium-hydrogen is dependent on the morphology of the palladium. There are a number of differences between the bulk forms of palladium that can contribute to this. Internal crystal temperatures may vary. The bulk form of palladium may have temperature gradients, which would cause concentration gradients. The different morphologies will have different methods of coping with dislocations. Powdered forms can more easily relieve dislocation stresses as the dislocations move to the surface and are annealed away.

A recent x-ray diffraction study by Suleiman *et al.* of nanometer sized palladium particles [20] shows that the physical form of palladium affects the lattice parameter. Suleiman *et al.* show that the pure palladium nano-particles have larger lattice parameters than bulk palladium, and that the individual sample morphology and the type of stabilizer used affects both the pure palladium lattice parameter and the rate of lattice expansion with hydrogen loading. They attribute this to the mechanical hardness of the stabilizer, but do not investigate the role of band structure on the processes. Different contaminants in palladium could produce similar effects as the different stabilizers in Suleiman *et al* if they are assumed to be electronic in nature. This would be more apparent with smaller particle morphology, as with the samples used in 2002 on SINQ HRPT and 2004 on ISIS HRPD, where trace contaminants will have a comparatively larger influence on the palladium band structure than in bulk forms.

Tang *et al.* [21] found that the palladium morphology affects the thermodynamic properties of the palladium-hydrogen system. The saturation solubility of hydrogen in the solid solution (alpha) phase and the absorption plateau pressure both increase with decreasing particle size, as is seen in the experiments presented here. They based this result on their own p-c-T measurements on palladium sponge samples, along with results from the literature.

The present diffraction study of October 2001 (HIFAR MRPD), was performed using a solid sheet of palladium as a sample. At 250°C both the p-c-T diagram and the refined lattice parameters show marked hysteresis. At 280°C there is no definitive hysteresis in either the p-c-T diagram or lattice parameters. At 300°C all traces of hysteresis have disappeared.

In the case of the powdered sample used in the studies of October 2003 (HIFAR HRPD) and March/April 2004 (ISIS HRPD), no trace of hysteresis is observable in the p-c-T isotherms collected at temperatures over 300°C (302 - 306°C and 310°C). Refinement of the patterns shows the presence of two separate lattice parameters and therefore two-phases, indicating that these temperatures are below the thermodynamic critical temperature.

The thermodynamic cause of the hysteresis in the sub-critical pressure loops of metal-hydrides is the loss of Gibbs free energy (ΔG_{loss}), which is directly related to the elastic strain in the system, and therefore the background dislocation density. Tang *et al.* show that ΔG_{loss} increases with particle size (see also [22]).

The temperature scan patterns from ISIS HRPD in April/May of 2004 (section 4.7.4) show that to fully anneal a palladium sample it must be held at 500°C at least for several hours.

Well below the critical temperature the onset of the two-phase region during hydrogenation is due to nucleation of β-phase amongst the α-phase, resulting in the discontinuous appearance of the beta-phase lattice parameter and eventual disappearance of the α-phase lattice parameter. Above the critical temperature, the process is a slow change from the alpha phase into the β-phase, with a corresponding constant linear increase in lattice parameter. As was shown in Chapter 4, the experiments of October 2003 on HIFAR HRPD and April/May 2004 on ISIS HRPD found two-phase lattice parameters at temperatures greater than any published thermodynamic critical temperature. The literature critical temperatures are based on the disappearance of hysteresis in the p-c-T isotherms. We have shown that there is a region where p-c-T thermodynamic two-phase behaviour is not detectable, but there are two distinct phase lattice parameters detectable via neutron diffraction.

In this intermediate region there exists two phases, which are almost identical. Both phases separately follow Vegard's Law and the lattice parameters do not appear discontinuously but

appear to bifurcate from the single-phase value This is different in behaviour from both the sub-critical and super-critical temperatures This region should properly be referred to as the *peri*-critical region of the palladium-hydrogen system, and is somewhere in the temperature range 300°C - 320°C (most likely 301°C - 315°C).

The phase diagram of the palladium-hydrogen system can be viewed as analogous to the liquid-gas transformation phase diagram for pure substances, where the critical temperature marks the point above which separate phases, liquid or gas, cannot co-exist The peri-critical effect, as shown in palladium-deuterium, would seem to have no analogy in the liquid-gas system as it is mediated by the palladium lattice and can only be detected by micro-structural investigations.

1. Yamada, M., Philosophical Magazine, 1922. **45**(265): p. 241-243
2. McKeehan, L.W., Physical Review, 1923. **21**: p. 334-342.
3. Kruger, F. and G. Geh, Ann. Phys., 1933. **16**: p. 174.
4. Rosenhall, G., Ann. Phys., 1933. **18**: p. 150.
5. Schirber, J.E. and B. Morosin, Physical Review B, 1975. **12**(1): p. 117-118.
6. Maeland, A.J. and T.R.P.jr. Gibbs, Journal of Physical Chemistry, 1961. **65**: p 1270.
7. Baranowski, B., S. Majchrzak, and T.B. Flanagan, Journal of Physics F: Metal Physics, 1971. **1**: p. 258-261.
8. Pitt, M.P. and E.M. Gray, Europhysics Letters, 2003. **64**(3): p. 344-350.
9. Rybalko, V.F., et al., Physics Letters A, 2001. **287**: p. 175-182.
10. Worsham, J.E., M.K. Wilkinson, and C.G. Shull, J. Phys. Chem. Solids, 1957. **3**: p. 303-310.
11. Mukhopdyay, R., et al., Solid State Communications, 1990. **75**(4): p. 359-362.
12. Vegard, L., Phys., 1921. **17**: p. 5.
13. Vegard, L., Z. Kristallogr, 1928. **67**: p. 239.
14. Bergsma, J. and J.A. Goedkoop, Physica, 1960. **26**: p. 744-750.
15. Hunter, B.A., Commission on Powder Diffraction Newsletter, 1998. **20**: p. 21.
16. Wicke, E. and J. Blaurock, Journal of the Less-Common Metals, 1987. **130**: p. 351-363.
17. Fukai, Y., *The Metal-Hydrogen System* Springer Series in Materials Science, ed H.K.V. Lotsch, et al. Vol. 21. 1993, New York: Springer-Verlag. 355.
18. Lewis, F.A., *The Palladium Hydrogen System*. 1967, Bungay: Academic Press 178.
19. Kisi, E., Personal communication 2004.
20. Suleiman, M., et al., Journal of Alloys and Compounds, 2005. **In Press**
21. Tang, T., S.-l. Guo, and G.-d. Lu, Materials Science Forum, 2005. **275-279**: p. 2485-2488.
22. Chen, W.C. and B.J. Heuser, Journal of Alloys and Compounds, 2000. **312**: p. 176-180